Atmos. Chem. Phys. Discuss., https://doi.org/10.5194/acp-2017-1007
Manuscript under review for journal Atmos. Chem. Phys.
Discussion started: 9 November 2017

Atmospheric Chemistry and Physics Discussions

How important are future marine and shipping aerosol emissions in warming Arctic summer and autumn?

Anina Gilgen[1], Wan Ting Katty Huang[1], Luisa Ickes[1,2], David Neubauer[1], and Ulrike Lohmann[1]

[1]ETH Zürich, Institute for Atmospheric and Climate Science, Switzerland
[2]Now at Stockholm University, Department of Meteorology, Sweden

Correspondence to: Anina Gilgen (anina.gilgen@env.ethz.ch)

Abstract. Future sea ice retreat in the Arctic in summer and autumn is expected to affect both natural and anthropogenic aerosol emissions: sea ice acts as a barrier between the ocean and the atmosphere, and reducing it increases dimethyl sulphide and sea salt emissions. A decrease in the area and thickness of sea ice could in addition lead to enhanced Arctic ship traffic, e.g. to shorten the paths of cargo ships. Changes in the emissions of aerosol particles can then influence cloud properties, precipitation, surface albedo, and radiation. Next to changes in aerosol particles, clouds will also be affected by increases in Arctic temperatures and humidities. In this study, we quantified how future aerosol radiative forcing, aerosol-cloud interactions, and cloud radiative effects might change in the Arctic in late summer (July/August) and early autumn (September/October).

Simulations were conducted for the years 2004 and 2050 with the global aerosol-climate model ECHAM6-HAM2. In 2050, simulations with and without additional ship emissions in the Arctic were carried out to quantify the impact of these emissions on the Arctic climate.

We found that aerosol number concentrations in the Arctic will generally increase in the future due to enhanced emissions of sea salt as well as dimethyl sulphide. The increase in cloud condensation nuclei will enhance cloud droplet number concentrations over the Arctic Ocean. Furthermore, both liquid and total water content will increase since the specific humidity will be enhanced due to higher temperatures and the exposure of the ocean's surface.

Changes in both aerosol radiative forcings and cloud radiative effects at the top of the atmosphere will not be dominated by the aerosol particles and clouds themselves but by the decrease in surface albedo (and by the increase in surface temperature for the longwave cloud radiative effect). Due to the reduction in sea ice, the aerosol radiative forcing will become less positive and the cloud radiative effect more negative, i.e. the cooling component of both will gain importance in the future.

We found that future Arctic ship emissions related to transport and oil/gas extraction (Peters et al., 2011, ACP) will not have a large impact on clouds and radiation: changes in aerosol concentrations only become significant when we increase these ship emissions by a factor of ten. The net aerosol radiative forcing shows only small, non-significant changes. Enhanced black carbon deposition on snow leads to a significant but very small warming over the central Arctic Ocean in early autumn. Furthermore, the tenfold higher ship emissions increase the optical thickness of low clouds and thus induce a small Twomey effect (cooling) in late summer. This Twomey effect has a considerably larger influence on temperature than the direct effect of particles (both aerosol particles in the atmosphere and particles deposited on snow), but it is more uncertain because of the

Atmos. Chem. Phys. Discuss., https://doi.org/10.5194/acp-2017-1007
Manuscript under review for journal Atmos. Chem. Phys.
Discussion started: 9 November 2017

Atmospheric Chemistry and Physics Discussions

large variability of clouds. In summary, future ship emissions might have a net cooling effect, which is small compared to other changes in future Arctic climate such as those caused by the decrease in surface albedo.

1 Introduction

Arctic temperatures increase approximately twice as fast as the global average temperature, partly due to temperature and ice-albedo feedbacks (Pithan and Mauritsen, 2014). This temperature increase has been leading to reductions in both Arctic sea ice extent and thickness for the last decades: for the period from November 1978 (start of satellite records) to December 2012, the Northern Hemisphere sea ice extent decreased by $3.8 \pm 0.3\,\%$ per decade (Vaughan et al., 2013). This decrease is more pronounced in summer and autumn than in winter and spring (Vaughan et al., 2013). Since Arctic temperatures will most likely increase further, the Arctic is expected to become ice-free in late summer within the next several decades (Collins et al., 2013; McFarquhar et al., 2011).

Sea ice concentration (SIC) refers to the percentage of an area which is covered with sea ice. Ocean areas with high SIC have a larger surface albedo and reduced exchanges of heat, momentum, and gases between the ocean and the atmosphere than areas with low SIC (Vaughan et al., 2013). With an open Arctic Ocean, natural aerosol emissions will increase because more sea salt particles and more dimethyl sulphide (DMS; a precursor for sulphate aerosol particles) will be emitted (Browse et al., 2014). Under present-day conditions, emissions from the ocean are already an important aerosol source in some Arctic regions in summer: measuring aerosol particles with radii between 0.25 to $10\,\mu\mathrm{m}$ in Svalbard, Deshpande and Kambra (2014) identified sea spray particles as the main source for Arctic summer aerosol particles. Note that a map of the Arctic, where some important land masses (such as Svalbard) and regional seas are labelled, can be found in the Appendix (Fig. A1). In a modelling study, Struthers et al. (2011) found that sea ice retreat might increase the sea salt aerosol number emissions in summer by a factor of two to three until 2100. In addition, sea ice retreat might also cause an increase in anthropogenic aerosol emissions over the Arctic Ocean, since reduced summer sea ice enables ships to pass through the Arctic Ocean. Cargo ships could shorten their paths, tourism (cruise ships) and fishery sectors could be expanded, and the Arctic oil and gas production will likely be intensified (Eckhardt et al., 2013; Peters et al., 2011). Nowadays, the Arctic air is exceptionally pristine and depleted of aerosols. Hence, increases in both natural and anthropogenic aerosol emissions might have a strong effect on cloud properties and radiation. Furthermore, deposition of black carbon (BC) on snow and ice lowers the surface albedo (Warren and Wiscombe, 1985) and therefore has the potential to accelerate sea ice retreat (Flanner, 2013).

Aerosol particles influence clouds e.g. by acting as cloud condensation nuclei (CCN) or ice nucleating particles (INPs). Freezing processes involving INPs are called heterogeneous freezing and can be subdivided into different heterogeneous freezing modes, among them contact freezing and immersion freezing (Vali, 1985); for a recent overview on heterogeneous freezing modes, see Kanji et al. (2017). The ability of an aerosol particle to act either as a CCN or an INP depends on its size and chemical composition (Boucher et al., 2013).

Hence, both aerosol concentration and composition influence cloud properties substantially (Boucher et al., 2013): at a constant liquid water amount, an increase in the number concentration of CCN changes the cloud droplet number concentration

(CDNC); it leads to more but smaller droplets, thus increasing the cooling effect of clouds ("Twomey effect"; Twomey, 1974, 1977). Since cloud droplets must reach a certain size before they form rain, this process may delay the formation of precipitation (Albrecht, 1989). On the other hand, an increase in aerosol concentrations could also lead to enhanced precipitation due to the presence of INPs, which reduce the required supercooling and/or supersaturation for ice initiation. An earlier freezing of some cloud droplets, followed by the Wegener-Bergeron-Findeisen process, may rapidly form cold precipitation (Lohmann, 2002). Aerosol-cloud interactions can affect cloud properties and the onset and/or intensity of precipitation further, as described e.g. in Lohmann and Feichter (2005); Jackson et al. (2012). In the Arctic, observations suggest that high aerosol concentrations decrease the number of precipitating particles by 1-2 orders of magnitude (Lance et al., 2011).

However, clouds are not only affected by aerosol particles. Increasing atmospheric temperatures are expected to shift the melting and the freezing levels – and thus also cloud ice – to higher altitudes. Additionally, higher temperatures will increase evaporation from the surface and, consequently, the available water vapour in the atmosphere. An open ocean further amplifies the increase in water vapour. Analysing satellite data from 2000 to 2010, Liu et al. (2012) found a negative correlation between sea ice extent and cloud cover over the Arctic Ocean, which was statistically significant and especially pronounced between July and November. Recently, Abe et al. (2016) showed with a coupled atmosphere-ocean model that enhanced heat and moisture fluxes resulting from the reduction in sea ice cover are indeed responsible for the simulated increases in cloud cover.

Both aerosol particles and clouds impact the Earth's radiation budget. Whether an aerosol particle predominantely absorbs or scatters radiation depends on its physical and chemical characteristics. Aerosol scattering of shortwave (SW) radiation tends to cool the atmosphere, whereas absorption and re-emission of SW and longwave (LW) radiation tend to warm it (Boucher et al., 2013). The sum of scattering and absorption is called extinction. Since the aerosol extinction (normalised by the aerosol mass) is generally largest when the size of the particle is comparable to the size of the wavelength, the SW effect is more important than the LW effect for the majority of atmospheric particles (Stier et al., 2007). However, for large particles such as dust or sea salt, LW effects can become relevant (Stier et al., 2007).

Similar to aerosol particles, clouds impact the Earth's radiation budget by absorption and re-emission of LW radiation (warming) and scattering and absorption of SW radiation (predominantly cooling). The absorption and re-emission of LW radiation depend on the water path, cloud temperature, cloud height, and the emissivity of the cloud (Chen et al., 2006; Alterskjær et al., 2010; Shupe and Intrieri, 2003). The scattering of SW radiation is a function of the number, size, and phase of the cloud particles, of the solar zenith angle, and of the surface albedo (Liou, 2002; Shupe and Intrieri, 2003).

Compared with the global mean, the SW radiative effect of Arctic clouds is less important because of the large solar zenith angle and the high surface albedo (Alterskjær et al., 2010). Therefore, the LW absorption of clouds becomes more important and generally exceeds the SW effect. Hence, Arctic clouds warm the planet in the annual average and show a net cooling effect only in summer (Walsh and Chapman, 1998). How Arctic clouds and their radiative effects will change in the future is still an open question. Generally, both the SW and the LW cloud radiative effect (CRE) are expected to become stronger. Palm et al. (2010) suggested that the overall effect of enhanced aerosol concentrations is to increase the net warming effect of Arctic clouds because LW radiation dominates in the long polar winter. In contrast, a modelling study of Alterskjær et al. (2010) found that the increase in anthropogenic aerosol emissions since pre-industrial times has led to larger changes in the

Atmos. Chem. Phys. Discuss., https://doi.org/10.5194/acp-2017-1007
Manuscript under review for journal Atmos. Chem. Phys.
Discussion started: 9 November 2017

Atmospheric Chemistry and Physics Discussions

annual Arctic SW (-0.85 $\mathrm{W\,m^{-2}}$) than in the LW (0.55 $\mathrm{W\,m^{-2}}$) CRE. However, their simulated LW radiation effect was approximately one order of magnitude smaller than suggested by the observation-based study of Garrett and Zhao (2006). Whereas Garrett and Zhao (2006) considered measurements from a specific location (near Barrow, Alaska) and analysed strong pollution events, Alterskjær et al. (2010) simulated the effect over the whole Arctic (defined as north of 71° N in their study) under all conditions. Other explanations for the different results include model uncertainties, especially regarding cloud cover and thin cloud frequency (Alterskjær et al., 2010). For Arctic summer, Mauritsen et al. (2011) showed that an increase in the number of aerosol particles can either decrease or increase the net CRE depending on the background aerosol concentration.

Using the global aerosol-climate model ECHAM6-HAM2, we aim to quantify the changes in future Arctic aerosol particles from both natural and anthropogenic sources. Furthermore, we analyse changes in clouds and radiation, which are partly caused by these changes in aerosol emissions. Our goal is to draw conclusions about how changes in radiative forcings and radiative effects may feed back on temperature; Fig. 1 provides a simplified overview of the most important interactions that can lead to possible temperature feedbacks. The model and the simulations, the boundary conditions, the emissions, and the used statistical method are described in Sect. 2. In the results and discussion section (Sect. 3), we will focus on the months July to October, when both the decrease in SIC and the increase in shipping through the Arctic Ocean will be most pronounced. In the conclusions (Sect. 4), our key findings will be summarised.

2 Methodology

2.1 ECHAM6-HAM2

2.1.1 General information about ECHAM6-HAM2

ECHAM6-HAM2 is the combination of the general circulation model ECHAM6 (Stevens et al., 2013) and the aerosol model HAM2 (Stier et al., 2005; Zhang et al., 2012). ECHAM6 solves prognostic equations for vorticity, divergence, surface pressure, and surface temperature and uses a flux form semi-Lagrangian transport scheme to advect water vapour, cloud liquid water, cloud ice, and trace components. HAM2 considers different aerosol species and different size modes. To link the simulated aerosol population with the CDNC and the ice crystal number concentration (ICNC), parameterisations for cloud droplet activation and ice nucleation were implemented (Abdul-Razzak and Ghan, 2000; Lohmann et al., 2008).

In HAM2, the aerosol components sulphate, BC, organic carbon (OC), sea salt, and mineral dust are considered (Zhang et al., 2012). The size distribution of the aerosol particles is described by four size ranges: the nucleation mode ($r_\mathrm{m} < 5\,\mathrm{nm}$; r_m is the mode radius of the aerosol particles), the Aitken mode ($5\,\mathrm{nm} < r_\mathrm{m} < 50\,\mathrm{nm}$), the accumulation mode ($50\,\mathrm{nm} < r_\mathrm{m} < 500\,\mathrm{nm}$), and the coarse mode ($r_\mathrm{m} > 500\,\mathrm{nm}$). Only a soluble mode exists for the nucleation mode, whereas a soluble/internally mixed and an insoluble mode exist for the other three size modes. Therefore, seven aerosol modes are considered in total, each described by a log-normal size distribution. Coagulation and condensation can shift aerosol particles to larger modes and/or from insoluble to internally mixed modes. Removal processes of aerosol particles in ECHAM6-HAM2 comprise wet deposition, dry deposition, and sedimentation.

Atmos. Chem. Phys. Discuss., https://doi.org/10.5194/acp-2017-1007
Manuscript under review for journal Atmos. Chem. Phys.
Discussion started: 9 November 2017

Atmospheric Chemistry and Physics Discussions

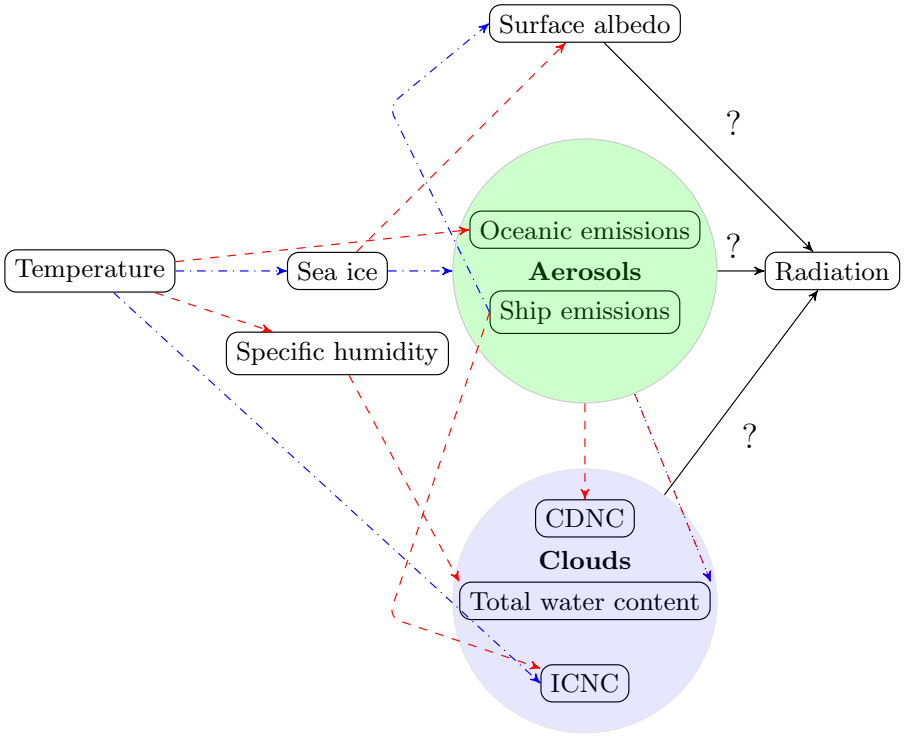

Figure 1. Simplified sketch showing how different variables (may) vary as a result of changes in Arctic temperatures. Red dashed arrows denote enhancing effects ("increase → increase" or "decrease → decrease"), blue dashdotted arrows dampening effects ("increase → decrease" or "decrease → increase"). For example, the future increase in Arctic temperature will lead to a decrease in sea ice concentration. Black solid arrows show which components impact radiation and therefore again temperature. Note that an increase in aerosol concentrations can either increase or decrease precipitation and thus the total water content, as mentioned in Sect. 1.

Regarding the sulphur chemistry, DMS is oxidised to SO_2 (sulphur dioxide), which can form sulphuric acid in the aqueous phase or in the gas phase. Gas-phase sulphuric acid in the atmosphere can either nucleate, i.e. form new small, soluble particles, or condense on pre-existing aerosol particles. Condensation can be limited by the available surface area of aerosol particles, by the available gas-phase sulphuric acid, or by the diffusion of the gas-phase sulphuric acid to the particle surface. If any gas-phase sulphuric acid is left after condensation, the sulphuric acid nucleates and forms new sulphate particles. Besides the available concentration of sulphuric acid, nucleation depends on temperature and relative humidity.

In the standard ECHAM6-HAM2 setup, a minimum CDNC of $40\,\mathrm{cm}^{-3}$ is implemented. This ensures that the global CDNC is not unrealistically low due to missing aerosol species in the model such as ammonium nitrate or due to the simplistic model description of organics. Since the Arctic is a remote, aerosol poor environment, the value $40\,\mathrm{cm}^{-3}$ is often undershot in this region (Bigg and Leck, 2001; Leaitch et al., 2016). Applying the standard CDNC threshold would drastically reduce the influence of changes in the CCN concentration and therefore impede aerosol-cloud interactions. Thus, we decided to use $10\,\mathrm{cm}^{-3}$ as a lower threshold for the CDNC everywhere.

Atmos. Chem. Phys. Discuss., https://doi.org/10.5194/acp-2017-1007
Manuscript under review for journal Atmos. Chem. Phys.
Discussion started: 9 November 2017

2.1.2 Aerosol emissions

Emissions of sea salt, dust, and oceanic DMS are calculated online and depend on the $10\,\mathrm{m}$ horizontal wind speed (u_{10}). Sea salt emissions follow Long et al. (2011) with sea surface temperature (SST) corrections according to Sofiev et al. (2011). Dust emissions are calculated as stated in Tegen et al. (2002), with some modifications based on Cheng et al. (2008). The monthly mean DMS seawater concentrations are prescribed according to Kettle and Andreae (2000), and the flux from the ocean to the atmosphere is calculated following Nightingale et al. (2000). Changes in oceanic DMS concentrations are not straightforward to project: taking primary production or SST as a proxy seems not justified since Arctic oceanic DMS concentrations also depend on taxonomic differences in phytoplanktonic assemblages (Becagli et al., 2016). Using a coupled ocean-atmosphere model (with ECHAM5-HAM as atmospheric component), the study by Kloster et al. (2007) explicitly simulates DMS but only reports changes between the time periods 2061-2090 and 1861-1890, which are not directly comparable to the time periods we are interested in. Thus, we decided to leave the oceanic DMS concentrations unchanged.

Besides dust, sea salt, and DMS, the emissions of all other aerosol components or precursors are prescribed, mainly from the ACCMIP emission inventory (Lamarque et al., 2010). For ship emissions, we used a different inventory, which is described in Sect. 2.3. Ship emissions are put into the second lowest model layer ($\approx 150\,\mathrm{m}$). While OC and BC particles from ships are exclusively emitted into the insoluble Aitken mode, the sulphate mass is equally distributed between the accumulation and the coarse mode. It is assumed that $2.5\,\%$ of SO_2 from ships is emitted as primary SO_4 (sulphate; Dentener et al., 2006).

2.1.3 Heterogeneous freezing of mixed-phase clouds in ECHAM6-HAM2

In ECHAM6-HAM2, BC particles emitted by ships can act as INPs. Heterogeneous freezing in ECHAM5-HAM is thoroughly described in the study of Hoose et al. (2008); more equations can be found therein. The only differences in ECHAM6-HAM2 are that i) only contact freezing by montmorillonite dust and immersion freezing by montmorillonite dust and BC are considered and that ii) only particles in the accumulation and coarse mode can induce freezing. The freezing rate is defined as number of cloud droplets that freeze per time and volume of air. Among other factors, the contact freezing rate depends on the volume-mean droplet radius as well as the CDNC, while the immersion freezing rate depends on the cloud water mixing ratio.

2.1.4 Calculation of aerosol radiative forcings and cloud radiative effects

Both aerosol radiative forcings and CREs are calculated online by calling the radiation scheme once with and once without considering aerosol particles or clouds (all-sky and clear-sky conditions, respectively); the difference between the two radiation calls is considered as the instantaneous aerosol radiative forcing or CRE. For SW radiation, aerosol radiative forcings and CREs both depend on the surface albedo. For example, an aerosol particle that scatters SW radiation can either have a cooling or a warming effect depending on whether the underlaying surface has a lower or a higher surface albedo, respectively. Since the surface albedo decreases in our future simulations due to melting of sea ice, changes in the radiative effects can either be caused by changes in aerosol/cloud properties or changes in surface albedo. For clouds, we can distinguish the two causes by applying the cloud radiative kernel method described in the study of Zelinka et al. (2012), which is independent of changes

in surface albedo. With this method, we can furthermore disentangle changes in LW CRE caused by changes in clouds from those caused by e.g. surface temperature changes. A higher surface temperature enhances the outgoing LW radiation from the surface. Thus, more LW radiation can be absorbed by clouds and the LW CRE increases. In addition, the cloud radiative kernel method allows for diagnosis of how different cloud types (low and free-tropospheric clouds; Zelinka et al., 2016) and changes in different cloud properties (cloud cover/amount, cloud optical thickness, and cloud top altitude) contribute to the total changes in CREs.

In our model, the reduction of snow albedo due to deposited BC is determined through interpolations of a lookup table based on a single-layer application of the SNICAR model (Flanner et al., 2007). The BC concentration in the top $2\,\mathrm{cm}$ of snow is considered. The concentration depends on the surface influx of snowfall as well as the influx of BC removed from the atmosphere through dry deposition, wet deposition, and sedimentation. Both BC scavenged by hydrometeors through in-cloud (Croft et al., 2010) and below-cloud (Croft et al., 2010) wet deposition are assumed to reach the surface within one timestep (if hyrometeors do not evaporate in subsaturated regions below clouds). Given that both the spatial and the temporal resolution of our model are low ($1.875° \times 1.875°$; $7.5\,\mathrm{min}$), this assumption seems justified. The concentration of BC in snow can be further modified through scavenging by snow melt and glacier runoff. Since the scavenging ratios are low (0.2 for BC particles in the internally mixed mode and 0.03 for those in the externally mixed mode; Flanner et al., 2007), the BC concentration in snow increases after snow melt. Lastly, while albedo reductions of snow on land and on sea ice are considered, the impact of BC deposition on bare sea ice is not. This is due to the different characteristics of the sea ice albedo concerning its interaction with the deposited BC, which would only lie on top of the ice instead of being mixed-in. However, as the spatial coverage of bare sea ice without any snow cover is small, the impact of omitting this darkening is expected to be negligible.

2.2 Model simulations

A summary of the model simulations can be found in Table 1. ECHAM6-HAM2 is an atmosphere-only model, i.e. SIC and SST need to be prescribed (see Section 2.4). To estimate the impact of future Arctic warming and sea ice retreat on aerosol particles and clouds, we conducted simulations under present-day (year 2004) and future (year 2050) conditions. The following simulations were performed with a resolution of T63L31 (corresponding to $\approx 1.875\,° \times 1.875\,°$ with 31 vertical levels):

- **arctic_2004**: Global greenhouse gas concentrations, SIC, SST, and ship emissions from the year 2004 are used.
- **arctic_2050_EM2004**: The global greenhouse gas concentrations in the year 2050 follow IPCC's Representative Concentration Pathway RCP8.5 (Collins et al., 2013). To prescribe future SIC and SST, we used results from an Earth System Model (ESM; see Section 2.4) simulation. The same prescribed aerosol emissions are used as in 2004. Therefore, all anthropogenic aerosol emissions between **arctic_2004** and **arctic_2050_EM2004** are identical.
- **arctic_2050**: The same as **arctic_2050_EM2004** but the prescribed aerosol emissions are representative for 2050. The emission factor of SO_2 ship emissions is smaller than in **arctic_2050_EM2004** since regulations and technological improvements are taken into account (see Sect. 2.3).

Atmos. Chem. Phys. Discuss., https://doi.org/10.5194/acp-2017-1007
Manuscript under review for journal Atmos. Chem. Phys.
Discussion started: 9 November 2017

Table 1. An overview of the different model simulations.

Model simulation	Greenhouse gas concentrations	SIC/SST	Anthropogenic aerosol emissions
arctic_2004	Year 2004	Year 2004	Year 2004
arctic_2050_EM2004	Year 2050	Year 2050	Year 2004
arctic_2050	Year 2050	Year 2050	Year 2050
arctic_2050_shipping	Year 2050	Year 2050	Year 2050 + additional ship emissions

– **arctic_2050_shipping**: The same as **arctic_2050** but with additional ship emissions in the Arctic. These emissions are estimated from Peters et al. (2011, see Section 2.3) based on future transport and oil/gas extraction. Since the impact of these additional Arctic ship emissions was hardly noticeable in our test simulations (not shown), we increased the emissions by a factor of ten (mass flux). By comparing **arctic_2050** with **arctic_2050_shipping**, we can estimate the impact of future Arctic ship emissions enabled by the smaller SIC.

Each simulation is run for 10 years with the same forcing for each year, therefore yielding 10 ensemble members.

2.3 Ship emission inventory

We used the ship emission inventory by Peters et al. (2011) for both present-day and future global ship emissions. It includes the species SO_2, BC, and OC for the years 2004, 2030, and 2050. For this study, we only use emissions from 2004 and 2050. The shipping emissions for the year 2004 are based on Dalsøren et al. (2009), who combined the observational data sets COADS and AMVER. Considering only ships above 100 gross tons, Dalsøren et al. (2009) found a total fuel consumption of 217 Mt for the year 2004.

Peters et al. (2011) used this 2004-inventory also as a "background" for the years 2030 and 2050. They assumed that emission factors of SO_2 will decrease due to regulations and improved technology but that everything else (other aerosol emission factors; shipping routes) will remain constant. In addition, Peters et al. (2011) calculated Arctic ship emissions for the years 2030 and 2050 for transit shipping and for shipping that is related to oil and gas production. Changes in ship emissions from the sectors tourism, fishery, and local/national transport are not considered. For the year 2004, no transit shipping was assumed, and the oil and gas shipping was estimated based on oil tankers operating in the Arctic region. The expected increase in these two sectors is related to SIC: less sea ice will faciliate the passage through the Arctic ocean and exploit new areas to oil and gas production. Peters et al. (2011) used different models to create their ship emission inventory; for more details we refer to their study. We processed the data from Peters et al. (2011) to create input files that are compatible with our model.

As mentioned previously, we increased ship emissions by a factor of ten to detect a noticeable signal in aerosol particles. This is in agreement with the results of Peters et al. (2014), who studied the effect of ship emissions on tropical warm clouds with ECHAM5-HAM. In the following, we explain why we consider the tenfold higher emissions to be an upper estimate of future Arctic ship emissions.

Atmos. Chem. Phys. Discuss., https://doi.org/10.5194/acp-2017-1007
Manuscript under review for journal Atmos. Chem. Phys.
Discussion started: 9 November 2017

Recently, McKuin and Campbell (2016) pointed out that both global and Arctic ship emission inventories might underestimate BC ship emissions because small fishing vessels ($< 100\,\mathrm{Gt}$) were not included in the analysis and because too low BC emission factors were used. In this study, we do not consider future changes in fishing activity. Therefore, both present-day and future background ship emissions should be underestimated by the same absolute amount in our analysis. If these background ship emissions were to occur over the Arctic Ocean or its vicinity, such an increase in background emissions might lead to a smaller impact of future transit and oil/gas related shipping (i.e. smaller relative increase of total aerosol emissions). This is an argument against increasing the Arctic ship emissions. A higher BC emission factor, on the other hand, would increase ship emissions from all sectors, although not necessarily by the same coefficient since BC ship emissions depend on engine and fuel type. While the ship emission inventory by Peters et al. (2011) used a BC emission factor of 0.35, McKuin and Campbell (2016) found – depending on the averaging method and the area (non-emission control versus emission control) – factors between 0.79 and 0.92. This suggests that $\approx$ 2.5 times higher BC ship emissions might be more appropriate for future transit and oil-gas-related shipping than the original estimate from Peters et al. (2011). Again, increases in background shipping emissions need to be considered as well.

Compared with other estimates of future Arctic transit shipping, the results from Peters et al. (2011) lie between those from Paxian et al. (2010) and Corbett et al. (2010): the fuel consumption by Paxian et al. (2010) is 1.4 to 2.4 times smaller than the values reported by Peters et al. (2011). Depending on the scenario, the estimated CO_2 emissions by Corbett et al. (2010) are 2 to 4.6 times higher in 2050 than the values reported by Peters et al. (2011).

Averaged over the period from July to October, transit shipping contributes more than petroleum-related shipping in the study from Peters et al. (2011), especially over the central Arctic Ocean. For transit shipping, the impact of ship emissions on climate is thus larger than for petroleum-related shipping since considerably higher emissions occur in regions where the background aerosol concentrations are lower.

Considering now that i) the BC emission factor used by Peters et al. (2011) is likely underestimated by a factor of $\approx$ 2.5, ii) transit shipping might be up to 4.6 times higher according to Corbett et al. (2010), and iii) transit shipping contributes most to the ship emissions over the aerosol-poor Arctic Ocean, increasing the additional ship emissions (both transit shipping and oil/gas related shipping) from Peters et al. (2011) by a factor of ten can be considered as realistic, though upper estimate. Furthermore, even if the tenfold higher ship emissions are probably too high to represent conditions in 2050, such high emissions could be reached in later years when population growth might lead to an increase in trade and petroleum demand.

2.4 Boundary conditions

Both SIC and SST are prescribed in ECHAM6-HAM2. For future conditions, we used model results from the Earth System Model MPI-ESM as input. We chose MPI-ESM because its atmospheric component is ECHAM and because the simulated future sea ice retreat is close to the model median of CMIP5. A drawback of our study is that we did not apply the mid-month correction to the MPI-ESM data as recommended by Taylor et al. (2000). Therefore, the seasonal variability in SIC and SST is somewhat underestimated. However, compared to the large differences in SIC and SST between 2004 and 2050, we do not expect this to affect the main conclusions of our study.

As mentioned previously, future greenhouse gas emissions follow the RCP8.5 scenario, which shows a similar CO_2 emission increase as the A2 scenario that Peters et al. (2011) assumed in their analysis. From 2004 to 2050, the global greenhouse gas volume mixing ratios change as follows: from 377 to 541 ppm for CO_2, from 1.76 to 2.74 ppm for CH_4, from 319 to 367 ppb for N_2O, from 256 to 107 ppt for CFC-11, and from 540 to 345 ppt for CFC-12 (CFCs are chlorofluorocarbons).

Since SIC and SST vary from year to year, we performed test simulations using SIC and SST from: i) the year 2003 and 2004 and ii) the first and the second ensemble member from the MPI-ESM CMIP5 simulation for the year 2050. Overall, the Arctic SIC in 2003 was somewhat smaller than in 2004, and the SIC in the first ensemble member from MPI-ESM was smaller than in the second ensemble member. However, we found that the basic results and main conclusions do not depend on these differences in SIC. In the following, we will therefore always refer to simulations using SIC and SST from 2004 and future SIC and SST from the first ensemble member of MPI-ESM. To verify consistency between future shipping routes and sea ice extent, we further compared the sea ice conditions used to calculate future ship emissions with the sea ice conditions employed in our simulations (Appendix B).

2.5 Statistical test

Wilks (2016) recently pointed out that the "naive stippling approach", which is commonly used in atmospheric sciences, leads to overstatements of scientific results: with the "naive stippling approach", a significance test is calculated for every gridpoint and all gridboxes are stippled where the p-value is smaller than 5 % (for a significance level of $\alpha = 0.05$). This approach has two main limitations: 1. Assuming that the spatial correlation is zero, 5 % of the gridboxes show on average stippling *just by chance*. 2. Spatial autocorrelation – often large when analysing gridded climate data – increases the false discovery rate (FDR) for the "naive stippling approach", i.e. the null hypothesis is often rejected although it is true. As suggested by Wilks (2016), we circumvent the problem by controlling the FDR instead. The advantages of this approach are the elimination of many spurious signals and the robustness concerning spatial correlation. In this method, a threshold p-value is calculated below which the result is supposed to be signal, not noise. We assume that the spatial correlation is moderate or large for the variables we are looking at. Therefore, we set α_{FDR} to $2 \times \alpha$ (see Wilks, 2016, for explanation). For the individual gridpoints, p-values are calculated using the Wilcoxon-Mann-Whitney test instead of the often used Welch's test since the latter is only valid if the samples are normally distributed (a condition which was sometimes not met in our results). The only exception where we used the Welch's test is for testing the significance of the results from the cloud radiative kernel method (see Appendix C): we could not apply the Wilcoxon-Mann-Whitney test to the cloud radiative kernel results because they are given as differences instead of absolute values.

3 Results and Discussion

First, the changes in natural aerosol populations, clouds, and their radiative forcings/effects in a warming Arctic will be assessed (Sect. 3.1). Second, we will determine the influence of additional Arctic shipping activity related to transit shipping and petroleum activites on climate (Sect. 3.2).

Atmos. Chem. Phys. Discuss., https://doi.org/10.5194/acp-2017-1007
Manuscript under review for journal Atmos. Chem. Phys.
Discussion started: 9 November 2017

Atmospheric Chemistry and Physics Discussions

Most figures will show the mean over the ten ensemble members for the reference simulation on the left and differences between the perturbed ensemble mean and the reference ensemble mean on the right. As mentioned previously, we will analyse the months July to October. Since the conditions (e.g. SW radiation, temperature) considerably change from July to October, averaging over these four months might hide significant changes occurring in only one or two months. Therefore, we decided to average the results from July to August (late summer) and from September to October (early autumn). If the season is not specified, results refer to both late summer and early autumn.

Each simulation consists of ten ensemble members to account for the high variability in Arctic climate. However, uncertainties associated with the used climate model can of course not be captured with this approach. It is well known that different global climate models considerably deviate, e.g. when simulating aerosol-cloud interactions. Furthermore, most models have problems to reproduce the structure of mixed-phase clouds prevalent in the Arctic, and the future sea ice extent as well as the prescribed aerosol emissions are highly uncertain. To gain a better understanding of the robustness of our results, we will compare them with other studies, both concerning relative and absolute changes.

3.1 Changes due to warming and sea ice retreat

In the following, we will analyse how future temperature increase in the Arctic affects natural aerosol particles, clouds, and radiation. For that, the simulation **arctic_2050_EM2004** will be compared with **arctic_2004**.

3.1.1 Aerosol particles

In the vicinity of the Arctic Ocean, both DMS and sea salt burdens significantly increase (not shown), which is predominantely caused by the decrease in SIC. As a second-order effect, significant increases in u_{10} over the central Arctic Ocean in early autumn increase sea salt and DMS emissions. Despite the pronounced increases in DMS burden, the sulphate burden does not change significantly since it is dominated by other emissions (e.g. anthropogenic SO_2 emissions). Also the aerosol size distributions at $950\,\mathrm{hPa}$ (Fig. 2a) and $800\,\mathrm{hPa}$ (Fig. 2b) show only small, non-significant changes from 2004 to 2050 (shown for early autumn; averaged between $70°$ to $90°\,\mathrm{N}$). The number concentration slightly increases in both the nucleation and the coarse mode. We attribute the enhanced number concentrations in the coarse mode mainly to direct sea salt emissions and the increase in the nucleation mode to DMS emissions; the latter is oxidised via SO_2 to sulphuric acid, which can form new particles. In early autumn, the number concentration decreases at $r_{\mathrm{ap}} \approx 0.1\,\mu\mathrm{m}$, which might be caused by (non-significant) decreases in BC and OC burdens.

Struthers et al. (2011) compared sea salt emissions for a nearly ice-free summer (2100) with present-day conditions (2000) and found an increase in mass emissions from $7.1\,\mu\mathrm{g m^{-2} s^{-1}}$ to $30.5\,\mu\mathrm{g m^{-2} s^{-1}}$ (factor of ≈ 4); this is an average over JJA (June, July, August) and 70-90° N. Note that we chose 2050 for our simulations due to the availability of Arctic ship emissions for this year. In the same region, Browse et al. (2014) found that sea salt emissions increased by a factor of 10 to $\approx 0.069\,\mu\mathrm{g m^{-2} s^{-1}}$ in August when comparing a hypothetically ice-free ocean with present-day conditions (2000). In our simulations, sea salt emissions increase from 1.48×10^{-3}/$2.43\times10^{-3}\,\mu\mathrm{g m^{-2} s^{-1}}$ (JJA/August) to 2.79×10^{-3}/$4.00\times10^{-3}\,\mu\mathrm{g m^{-2} s^{-1}}$ from 70-90° N in 2050, i.e. by a factor of < 2. As expected, the relative increase in emissions is largest in the study by Browse

Atmos. Chem. Phys. Discuss., https://doi.org/10.5194/acp-2017-1007
Manuscript under review for journal Atmos. Chem. Phys.
Discussion started: 9 November 2017

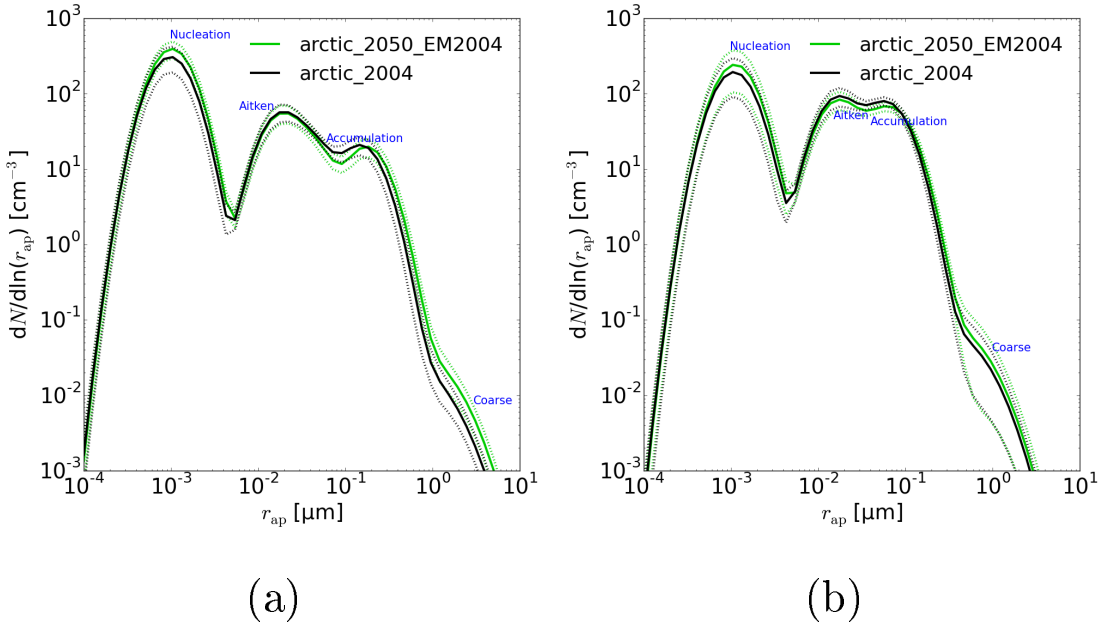

Figure 2. Aerosol number size distributions in 2004 (**arctic_2004**) and 2050 (**arctic_2050_EM2004**); N stands for the number concentration, r_{ap} for the radius of the aerosol particles. The size distributions are shown for early autumn (Sep/Oct) at 950 hPa (a) and 800 hPa (b), averaged between 70° and 90° N. The solid lines denote ensemble means, the dotted lines the subtracted/added standard deviations. Different colors (black, green) stand for different simulations (see legend).

et al. (2014), where the absolute decrease in SIC is largest, and smallest in our study, where the absolute decrease in SIC is smallest. Present-day emissions are a factor of $\approx$ 3 lower in our simulations compared with Browse et al. (2014), which results from the differences in the two parameterisations (modified Long et al., 2011; Gong, 2003) as shown in the study of Long et al. (2011). The absolute emissions reported by Struthers et al. (2011) are at least three orders of magnitudes higher than in our simulations. This might again be caused by the parameterisations used since differences in u_{10} and SST are too small to explain the large disagreement. Struthers et al. (2011) used a modification of the Mårtensson parameterisation combined with the Monahan parameterisation for particles $> 1.4\,\mu\mathrm{m}$ (Mårtensson et al., 2003; Monahan et al., 1986). However, neither Long et al. (2011) using the Mårtensson parameterisation nor us using the Monahan parameterisation for particles $r_{\mathrm{dry}} < 4\,\mu\mathrm{m}$ (in earlier simulations with ECHAM-HAM; not shown) found as high emissions as Struthers et al. (2011). Therefore, we expect that differences in the number fluxes of large particles ($> 4\,\mu\mathrm{m}$), which contribute most to mass emissions (Long et al., 2011), are responsible for the large discrepancy.

Atmos. Chem. Phys. Discuss., https://doi.org/10.5194/acp-2017-1007
Manuscript under review for journal Atmos. Chem. Phys.
Discussion started: 9 November 2017

3.1.2 Clouds

Except for cloud cover, the averages of cloud properties (such as liquid water content or CDNCs) refer to in-cloud values, i.e. by averaging only over periods and locations when and where clouds are present.

In general, the number of aerosol particles acting as CCN increases in future, which leads to enhanced CDNCs (shown in Fig. 3d for early autumn). Also the liquid water content increases (see Fig. 3b) because both the open ocean and higher air temperatures increase the specific humidity. The increase in liquid water content can be ascribed to both higher CDNCs and larger cloud droplets. Precipitation shows no significant changes.

We also obtain increases CDNCs (which we attribute to increases in CCN concentrations) when averaging over cloudy and non-cloudy conditions. In contrast, Browse et al. (2014) found small decreases in CCN concentrations (averaged over cloudy and non-cloudy conditions) over the Arctic Ocean. In their simulations, the liquid clouds over the ocean suppressed new particle formation via aqueous phase oxidation of SO_2 (a process also considered in ECHAM6-HAM2). Instead, particles grew to larger sizes and were efficiently scavenged by drizzle. The different responses when compared to our simulations could e.g. be caused by different oxidant concentrations (H_2O_2, O_3) or by the different handling of drizzle and precipitation: Browse et al. (2014) derived drizzle rates from Arctic observations of cloud altitude and droplet concentrations and scaled them by the low-cloud fraction. On the other hand, cloud microphysical processes (e.g. diffusional growth, coagulation) are explicitly calculated in our simulations and coupled with aerosol particles via Köhler theory and freezing parameterisations. Drizzle is not considered as a separate size class in our simulations; however, Sant et al. (2015) have shown with ECHAM5-HAM that the impact of drizzle on the CDNC burden is rather small in the Arctic.

As expected, the higher temperatures in 2050 influence the occurrence of cloud ice (both cirrus and mixed-phase) in our simulations by shifting the isotherms and thus also cloud ice towards higher altitudes. Changes in ice water content (Fig. 4b) can be caused by changes in the ICNC (Fig. 4d) and/or the effective ice crystal radius (Fig. 4f). At altitudes below $500\,\mathrm{hPa}$, both changes in the ICNC and radius have an influence. The increase of ICNC near the surface is due to the increase in CDNC. Between $500\,\mathrm{hPa}$ and $200\,\mathrm{hPa}$, the enhanced ice water content is linked to the increase in ice crystal radius.

Especially in early autumn, significant changes in cloud cover occur (see Fig. 5). Cloud cover decreases where precipitation is most enhanced (near Svalbard) but increases over the East Siberian Sea and the Beaufort Sea where sea ice has vanished (Fig. A1 shows a map of the Arctic Ocean where the regional seas are labelled). The latter is consistent with the findings from Abe et al. (2016), who found increases in the October cloud cover caused by sea ice reduction (which leads to an enhanced moisture flux to the atmosphere).

Atmos. Chem. Phys. Discuss., https://doi.org/10.5194/acp-2017-1007
Manuscript under review for journal Atmos. Chem. Phys.
Discussion started: 9 November 2017

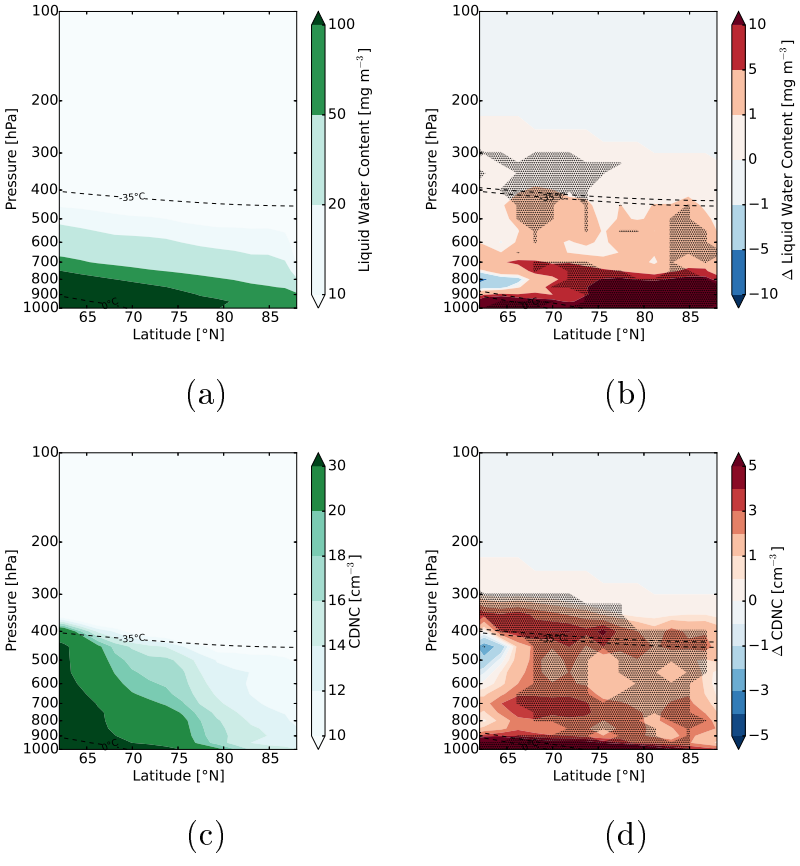

Figure 3. Liquid water content and CDNC in 2004 in (a)/(c) and differences between 2050 and 2004 (i.e. between simulations **arctic_2050_EM2004** and **arctic_2004**) in (b)/(d) (all when/where clouds are present) in early autumn (Sep/Oct). Stippled areas are significant at the 95% confidence level. The dashed lines show the 0°C- and the -35°C-isotherms (for both 2004 and 2050 for the difference plots).

Atmos. Chem. Phys. Discuss., https://doi.org/10.5194/acp-2017-1007
Manuscript under review for journal Atmos. Chem. Phys.
Discussion started: 9 November 2017

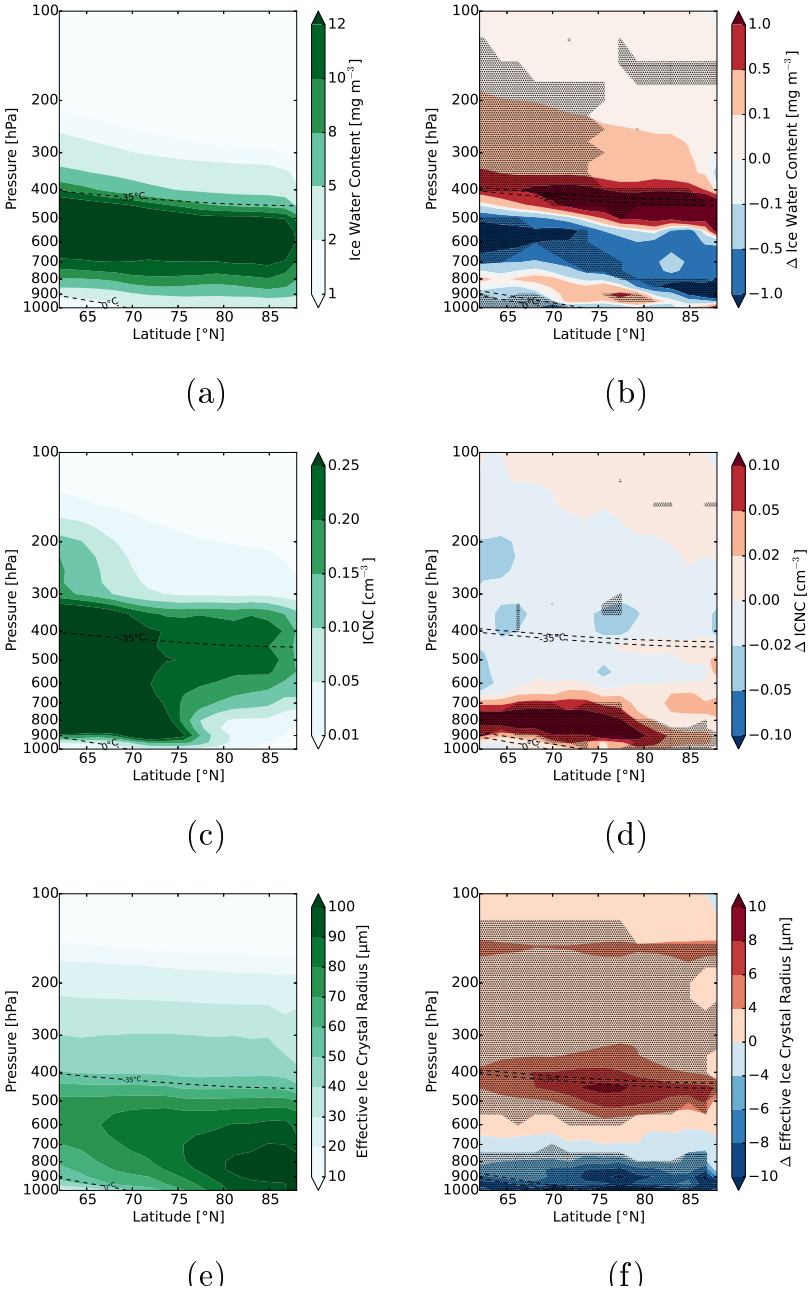

Figure 4. Ice water content, ICNC, and effective ice crystal radius in 2004 in (a)/(c)/(e) and differences between 2050 and 2004 (i.e. between simulations **arctic_2050_EM2004** and **arctic_2004**) in (b)/(d)/(f) (all when/where clouds are present) in early autumn (Sep/Oct). Stippled areas are significant at the 95% confidence level. The dashed lines show the 0°C- and the −35°C-isotherms. Note that they are zonally and temporally averaged, hence ice can exist at altitudes below the 0°C-isotherm.

Atmos. Chem. Phys. Discuss., https://doi.org/10.5194/acp-2017-1007
Manuscript under review for journal Atmos. Chem. Phys.
Discussion started: 9 November 2017

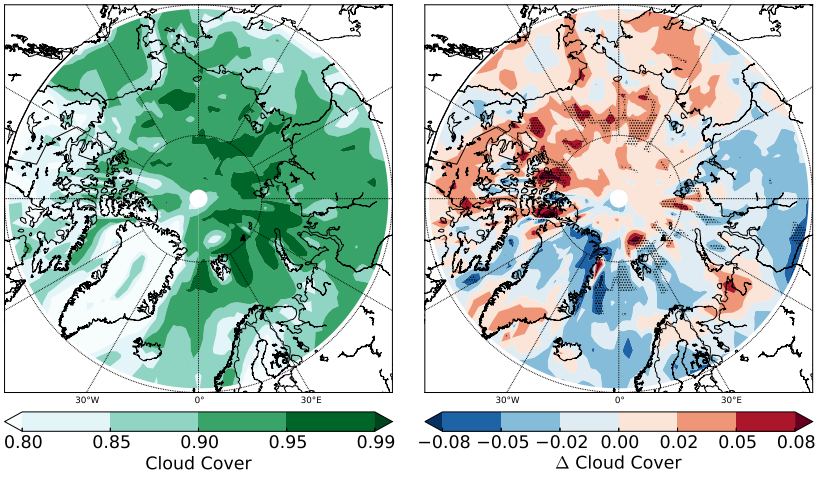

Figure 5. (a) Cloud cover in 2004 and (b) differences between 2050 and 2004 (i.e. between simulations **arctic_2050_EM2004** and **arctic_2004**) in early autumn (Sep/Oct). Stippled areas are significant at the 95% confidence level.

3.1.3 Aerosol radiative forcings

Unless otherwise stated, all radiative forcings and radiative effects refer to those at the top of the atmosphere (TOA). In 2004, aerosol particles cool the Arctic under clear-sky conditions (i.e. absence of clouds), except over the Arctic Ocean and Greenland, where the surface albedo is high (see Fig. 6c). If the presence of clouds is considered, aerosol particles warm the atmosphere also over Alaska and northeast Siberia (late summer) and over the whole northern Russia (early autumn; shown in Fig. 6e). Part of this warming might be caused by absorbing aerosol layers lying above clouds (not shown): since the clouds reflect more SW radiation than the snow/ice-free surface, more SW radiation can be absorbed by aerosol particles. Moreover, the scattering of aerosol particles could become less important in the presence of clouds, which increases the relative importance of aerosol absorption to extinction. Averaged over the whole Arctic region, aerosol particles have a cooling effect under clear-sky conditions in 2004 but a warming effect if clouds are considered. Note that changes at the surface are of opposite sign, i.e. the aerosol particles cool the surface under all-sky conditions. In our simulations, both the cooling and the warming are more pronounced in late summer than in early autumn due to the higher availability of SW radiation.

Increases in DMS and sea salt burdens lead to significant increases in aerosol optical thickness (AOT) in 2050, which are expected to induce a cooling since sea salt and sulphate particles are nearly pure scatterers. We cannot disentangle the aerosol radiative forcing induced by surface albedo changes from that induced by AOT changes. However, comparing aerosol radiative forcings over regions where the surface albedo has not decreased – e.g. over the Norwegian Sea, the Greenland Sea, and the Barents Sea – shows that the increases in natural aerosol particles indeed lead to a significant cooling independent of surface albedo changes (compare Fig. 6b, f). Therefore, both changes in surface albedo and in AOT increase the net cooling effect of

aerosol particles under clear-sky conditions and decrease the net warming effect under all-sky conditions in the Arctic region. When we compare our results with those by Struthers et al. (2011, averaged over 70-90° N, JJA), we find that the absolute changes in aerosol-radiation interactions are similar despite the different absolute values: while Struthers et al. (2011) report a decrease in the direct aerosol radiative forcing from -0.085 (2000) to $-0.252\,\mathrm{Wm^{-2}}$ (2100), we find a decrease from 0.476 (2004) to $0.287\,\mathrm{Wm^{-2}}$ (2050). Our values refer to all aerosol particles, those of Struthers et al. (2011) on the other hand only to natural aerosol particles (defined by them as sea salt and mineral dust). This at least partially explains the discrepancy in absolute values since strongly absorbing BC particles are only included in our estimates.

The radiative forcing due to BC deposition on snow decreases significantly because less snow-covered sea ice and less snow on land exist. However, the radiative forcing due to deposited BC as well as its absolute changes are small compared to other radiative forcings (significant decreases are always below $0.05\,\mathrm{Wm^{-2}}$). This is also displayed in Tables 2 and 3, which show the area-averaged absolute differences in radiative forcings north of 60° N and north of 75° N, respectively.

3.1.4 Cloud radiative effects

Not only the aerosol radiative forcing but also CREs change significantly. Using the radiative kernel method, we first assess how CREs change only as a function of cloud properties (i.e. independent of changes in e.g. surface albedo or temperature). In this case, we find no significant changes in late summer. In early autumn, changes in SW CRE are not significant when averaged over latitudes between 60°/75° and 90° N (see Tables 2, 3). However, the SW CRE shows locally significant changes, e.g. decreases over the central Arctic Ocean or increases along the west coast of Greenland (Fig. 7c), which match the changes in cloud cover in Fig. 5. In contrast, changes in LW CRE are not significant, neither for individual gridboxes nor when spatially averaged (Fig. 7f, Tables 2, 3).

If we use the standard method for calculating CREs, which considers also impacts due to changes in surface albedo and surface temperature, changes in both SW and LW CRE are much more pronounced over the central Arctic Ocean in early autumn than with the radiative kernel method (Fig. 7b, e). Similarly to aerosol particles, the large changes in SW CRE are mainly caused by the smaller surface albedo (i.e. larger changes in Fig. 7b than in Fig. 7c). In contrast, increases in LW CRE primarly result from increases in surface temperature. The decrease of LW CRE over the Bering Sea (which only occurs in Fig. 7e and not in Fig. 7f) can also be explained by changes in surface temperature (a decrease in this case). Due to the ice-albedo-feedback, decreases in surface albedo are highly correlated with increases in surface temperature over the Arctic Ocean. Furthermore, changes in cloud cover and thickness affect both SW and LW CRE. Changes in SW and LW CRE thus mostly occur at the same locations. Since they are of opposite sign and on the same order of magnitude, they cancel to a large degree, and the net CRE in early autumn shows no significant changes.

In late summer, the net CRE decreases significantly, i.e. the cooling effect of clouds increases. This is because i) the SW component dominates in these months due to the higher zonal zenith angle and ii) the surface temperature over the central Arctic Ocean does not show pronounced increases like in early autumn (more sea ice available), therefore not enhancing the LW CRE.

Atmos. Chem. Phys. Discuss., https://doi.org/10.5194/acp-2017-1007
Manuscript under review for journal Atmos. Chem. Phys.
Discussion started: 9 November 2017

Atmospheric Chemistry and Physics Discussions

Compared with the results by Struthers et al. (2011), our changes in the SW CRE are rather small: averaged between 70° and 90° N (JJA), the radiative effect increases from -63.7 to $-107.7\,\mathrm{Wm^{-2}}$ (i.e. change by $-44\,\mathrm{Wm^{-2}}$) and from -48.0 to $-55.6\,\mathrm{Wm^{-2}}$ (i.e. change by $-7.6\,\mathrm{Wm^{-2}}$) in their and our simulations, respectively. The larger relative change reported by Struthers et al. (2011) is likely caused by the larger decrease in SIC: while still considerable parts of the Arctic Ocean are covered by sea ice in our simulations in 2050 (especially in July), only little sea ice is left in the simuations by Struthers et al. (2011) in 2100.

To investigate which absolute estimate of SW CRE might be more appropriate, we compared the simulated present-day CREs from Struthers et al. (2011) and our study with the ones derived by Intrieri et al. (2002) and Shupe and Intrieri (2003), which are based on the measurements from the Surface Heat Budget of the Arctic (SHEBA) campaign. The SHEBA campaign took place in the Beaufort and Chukchi Seas from October 1997 to October 1998. Intrieri et al. (2002) and Shupe and Intrieri (2003) reported values for CREs at the surface, but since the SW CREs at the TOA and at the surface are fairly similar (Laszlo and Pinker, 1993; Mauritsen et al., 2011; Wild et al., 2017), we expect a resembling absolute bias at the TOA. From June to August, our simulated values in the region of the SHEBA campaign are for each month $\approx 20\,\mathrm{Wm^{-2}}$ more negative than the results by Intrieri et al. (2002) and Shupe and Intrieri (2003). This indicates that our SW CRE might be overestimated, whereas the LW CRE is in good agreement. Provided that the results from the SHEBA campaign are also representative for other Arctic regions and other years than 1998, this suggests that the SW CRE by Struthers et al. (2011) would be even more overestimated than in our simulations.

Atmos. Chem. Phys. Discuss., https://doi.org/10.5194/acp-2017-1007
Manuscript under review for journal Atmos. Chem. Phys.
Discussion started: 9 November 2017

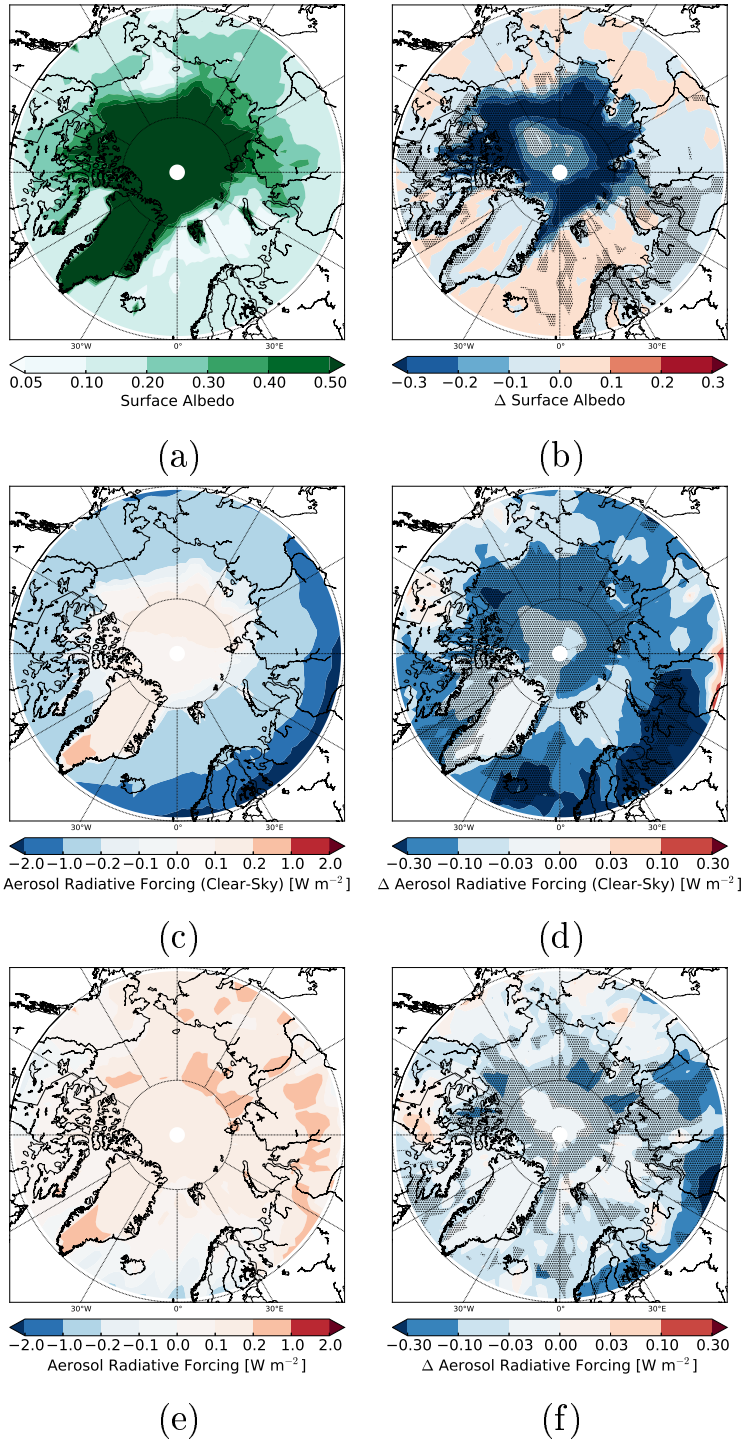

Figure 6. Surface albedo, aerosol net radiative forcing (clear-sky), and aerosol net radiative forcing (all-sky) in 2004 in (a)/(c)/(e) and differences between 2050 and 2004 (i.e. between simulations **arctic_2050_EM2004** and **arctic_2004**) in (b)/(d)/(f) in early autumn (Sep/Oct). Stippled areas are significant at the 95% confidence level.

Atmos. Chem. Phys. Discuss., https://doi.org/10.5194/acp-2017-1007
Manuscript under review for journal Atmos. Chem. Phys.
Discussion started: 9 November 2017

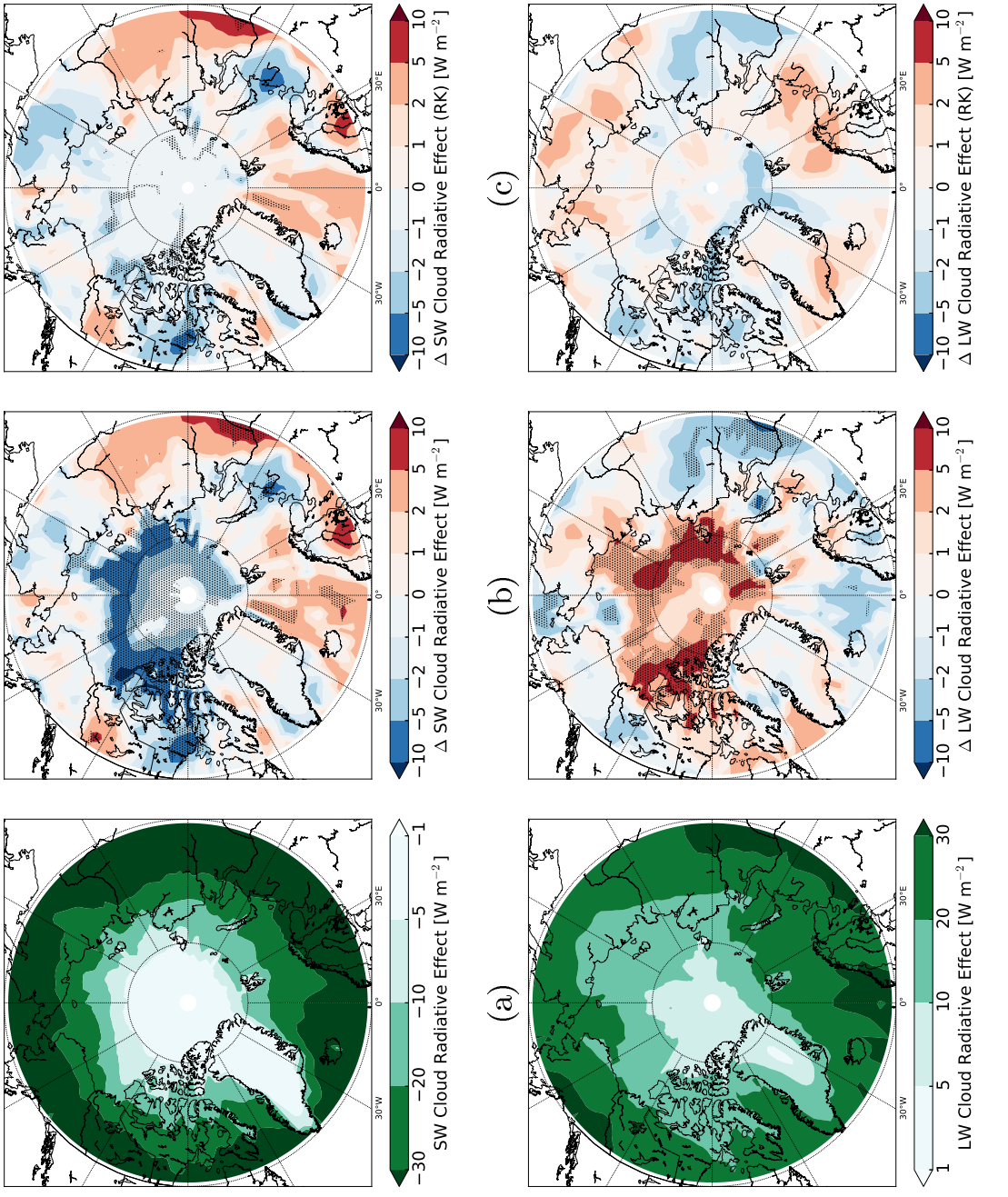

Figure 7. SW and LW CRE in 2004 in (a)/(d) and differences between 2050 and 2004 (i.e. between simulations **arctic_2050_EM2004** and **arctic_2004**) in (b)/(c)/(e)/(f) in early autumn (Sep/Oct). In (b) and (e), the changes in CREs were calculated online from two radiation calls (once with, once without clouds). In (c) and (f), the changes in CREs were calculated with the radiative kernel (RK) method, which does not depend on e.g. changes in surface albedo and surface temperature. Stippled areas are significant at the 95% confidence level.

Atmos. Chem. Phys. Discuss., https://doi.org/10.5194/acp-2017-1007
Manuscript under review for journal Atmos. Chem. Phys.
Discussion started: 9 November 2017

Atmospheric Chemistry and Physics Discussions

Table 2. Differences in radiative forcings (in $\mathrm{W\,m^{-2}}$) averaged over all latitudes north of 60° N in late summer (Jul/Aug) and early autumn (Sep/Oct). **arctic_2050_EM2004−arctic_2004** accounts for changes between 2050 and 2004 associated with a warmer climate, which leads to a reduction in sea ice concentration and therefore increased natural aerosol emissions. **arctic_2050_shipping−arctic_2050** considers the impact of an increase in future Arctic ship emissions in 2050. RK stands for radiative kernel method (see text for details). The star (*) denotes changes that are significant at $\alpha = 5\,\%$.

	Late summer "Warmer climate" (**arctic_2050_EM2004−arctic_2004**)	Late summer "Ship emissions" (**arctic_2050_shipping−arctic_2050**)	Early autumn "Warmer climate" (**arctic_2050_EM2004−arctic_2004**)	Early autumn "Ship emissions" (**arctic_2050_shipping−arctic_2050**)
Net SW radiation	4.31*	-0.85	0.94	-0.26
Net LW radiation	0.67	-0.30	-2.05*	-0.38
Aerosols	-0.089*	-0.005	-0.051*	0.006
BC deposition	-0.005	0.018*	0.005	0.010*
Clouds SW	-3.29*	-0.99	-0.41*	-0.28
Clouds LW	-0.17	-0.16	0.50	-0.36
Clouds SW (RK)	-1.06	-1.05	0.07	-0.29
Clouds LW (RK)	-0.63	-0.18	-0.01	-0.31

Table 3. The same as Table 2 but for differences in radiative forcings (in $\mathrm{W\,m^{-2}}$) averaged over all latitudes north of 75° N.

	Late summer "Warmer climate" (**arctic_2050_EM2004−arctic_2004**)	Late summer "Ship emissions" (**arctic_2050_shipping−arctic_2050**)	Early autumn "Warmer climate" (**arctic_2050_EM2004−arctic_2004**)	Early autumn "Ship emissions" (**arctic_2050_shipping−arctic_2050**)
Net SW radiation	12.95*	-1.25	2.77*	-0.32
Net LW radiation	0.93	-0.53	-4.38*	-0.13
Aerosols	-0.162*	0.018	-0.042*	0.011*
BC deposition	-0.045*	0.034	0.003	0.009
Clouds SW	-9.56*	-2.06	-2.15*	-0.36
Clouds LW	-0.02	-0.13	2.44*	-0.20
Clouds SW (RK)	-1.52	-1.99	-0.30	-0.37
Clouds LW (RK)	0.62	0.03	-0.38	0.11

Atmos. Chem. Phys. Discuss., https://doi.org/10.5194/acp-2017-1007
Manuscript under review for journal Atmos. Chem. Phys.
Discussion started: 9 November 2017

3.2 Impact of additional ship emissions

Future sea ice retreat will enable ships to pass through the Arctic Ocean, thus likely leading to enhanced shipping activity in late summer and early autumn. In this section, we will study the influence of these anthropogenic aerosol emissions on aerosol populations, clouds, and their radiative forcings/effects by comparing the simulation **arctic_2050_shipping** with **arctic_2050**.

3.2.1 Aerosol particles

Due to the increase in Arctic ship emissions (tenfold increase of the ship emissions by Peters et al. (2011) in 2050), the burdens of BC and SO_4 are significantly enhanced in late summer. In early autumn, rises in ship-related aerosol burdens are even more pronounced and also significant for OC. The increases in burden (see Fig. 8b) occur at the same locations as the ship emissions (see Fig. 8c), as shown for the example of BC. While the changes in natural aerosol emissions (2050 versus 2004) only have a minor influence on the number size distribution (Fig. 2), the impact of increased ship emissions is considerably larger. Figure 9 shows the aerosol number size distributions averaged between 70° and 90° N, at both $950\,\mathrm{hPa}$ (corresponding to $\approx 540\,\mathrm{m}$ using the hypsometric equation; Fig. 9a) and $800\,\mathrm{hPa}$ (corresponding to $\approx 1950\,\mathrm{m}$; Fig. 9b) for early autumn. At $950\,\mathrm{hPa}$, the number of particles in the nucleation mode decreases, whereas it increases in the accumulation mode (Fig. 9a). For the Aitken mode, a slight decrease and a distinct increase occur in late summer (not shown) and early autumn, respectively. At $800\,\mathrm{hPa}$, the effect of ship emissions on the aerosol size distribution is smaller than at $950\,\mathrm{hPa}$ (Fig. 9b). In addition to slight changes in the other three size modes, the number of coarse mode particles increases. However, for the coarse mode, the standard deviation is much larger at $800\,\mathrm{hPa}$ than near the surface, which makes this increase very uncertain.

We hypothesise that the additional aerosol particles emitted by ships provide additional surfaces for the condensation of gaseous sulphuric acid, which suppresses nucleation and thus decreases the number concentration of particles in the nucleation mode. The number concentrations in the other three size modes increase both by direct emissions and by shifting aerosol particles to larger sizes due to coagulation and condensation. Since ship emissions occur near the surface, the influence at $800\,\mathrm{hPa}$ is much smaller than at $950\,\mathrm{hPa}$.

3.2.2 Clouds

Although ship emissions have a larger effect on aerosol burdens and size distributions in early autumn than in late summer, significant aerosol-induced changes in clouds only occur in late summer. In the following, we will therefore only discuss results for late summer. The impact is mainly restricted to liquid clouds near the surface over the Arctic Ocean. Consistent with the Twomey effect, the CDNC increases and the effective radius decreases with additional ship emissions (see Fig. 10). Overall, the increase in CDNC contributes more to the cloud water mass than the decrease in cloud droplet radius, leading to a somewhat enhanced liquid water content.

Using satellite data, Christensen et al. (2014) studied the effect of ship tracks on both mixed-phase and liquid clouds. In late summer 2050, the clouds that are impacted by ships in our simulations are mostly liquid. Therefore, we restrict our comparison to the influence of ships on liquid clouds. Consistent with our results, Christensen et al. (2014) found decreases in the effective

Atmos. Chem. Phys. Discuss., https://doi.org/10.5194/acp-2017-1007
Manuscript under review for journal Atmos. Chem. Phys.
Discussion started: 9 November 2017

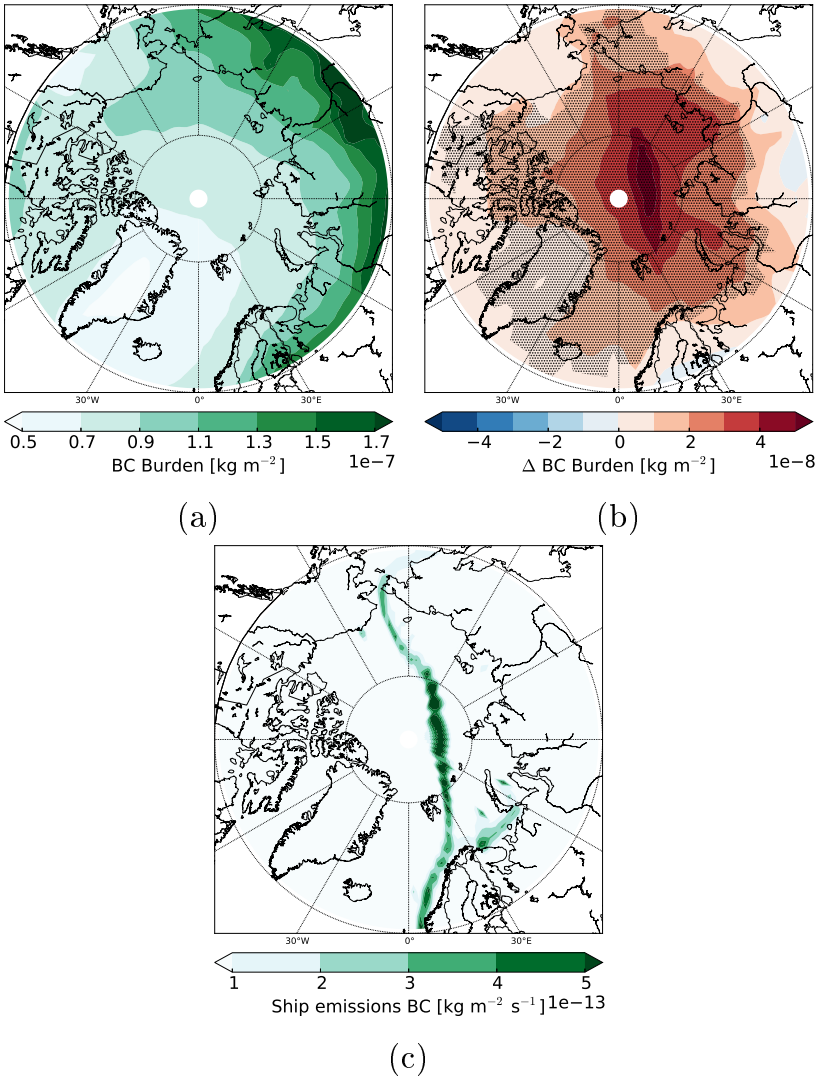

Figure 8. Panel (a) shows the BC burden in 2050 without considering enhanced Arctic ship emissions. Panel (b) shows the difference between a simulation with additional Arctic ship emissions and a simulation without these emissions in 2050 (difference between **arctic_2050_shipping** and **arctic_2050**). Stippled areas are significant at the 95% confidence level. Panel (c) shows tenfold higher (transit and petroleum-related) ship emissions of BC in 2050 based on the emission inventory by Peters et al. (2011). All values are for early autumn (Sep/Oct).

radius and increases in cloud optical thickness. The liquid water content slightly decreases in their analysis; in contrast, it slightly increases in our simulations. While our simulated precipitation shows no clear trend, the results by Christensen et al. (2014) suggest that ship emissions delay precipitation by enhancing cloud lifetime. The different results could be explained by

Atmos. Chem. Phys. Discuss., https://doi.org/10.5194/acp-2017-1007
Manuscript under review for journal Atmos. Chem. Phys.
Discussion started: 9 November 2017

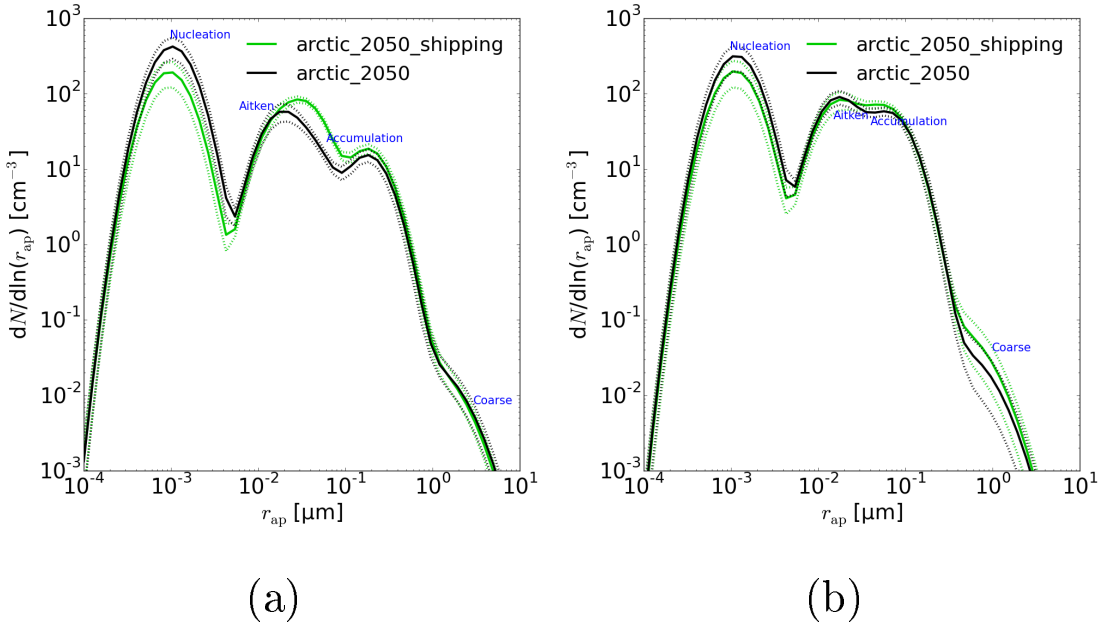

Figure 9. The impact of additional future ship emissions (**arctic_2050_shipping** versus **arctic_2050**) on aerosol number size distributions; N stands for the number concentration, r_{ap} for the radius of the aerosol particles. The size distributions are shown for early autumn (Sep/Oct) at $950\,\mathrm{hPa}$ (a) and $800\,\mathrm{hPa}$ (b), averaged between 70° and 90° N. The solid lines denote ensemble means, the dotted lines the subtracted/added standard deviations. Different colors (black, green) stand for different simulations (see legend).

the location of the ship tracks analysed by Christensen et al. (2014): the majority of their samples lie between 45° S and 45° N, and only very few datapoints are from the Arctic. Precipitation formation at high and low latitudes differs considerably since e.g. convection is usually much more important at low latitudes.

While liquid clouds are significantly impacted by ships in our simulations, this is not the case for cloud ice. Theoretically, ship emissions could influence heterogeneous freezing in ECHAM6-HAM2 by several processes, for example:

- The increase in BC emissions could lead to enhanced immersion freezing by BC.
- The increased SO_2 emissions could shift some dust particles from the insoluble to the internally mixed mode, which shifts contact freezing to immersion freezing, i.e. to colder temperatures (as found by e.g. Hoose et al., 2008).
- Decreases in the droplet radius would decrease the contact freezing rate.
- Increases in the CDNC would increase the contact freezing rate.

The last two effects might partly cancel each other since a larger number concentration of CCN is expected to simultaneously decrease the droplet radius and increase the CDNC. However, also the first two points seem to be irrelevant as ship emissions

have no significant impact on ice clouds in our simulations. To better understand why and gain some insights into the importance of the different heterogeneous freezing processes, we calculated the number of ice crystals that freeze in each of these processes (Fig. 11a, c, e). Immersion freezing by dust is the dominant freezing process in the Arctic (Fig. 11c). However, contact freezing by dust is more important near the surface since it can induce freezing at higher temperatures than immersion freezing (Fig. 11a). With additional ship emissions, the number of ice crystals formed by contact freezing decreases near the surface and increases at higher altitudes (Fig. 11b). Since the relative changes in CDNC are larger than the relative changes in droplet radius (which would increase the contact freezing rate), we suspect that contact freezing near the surface is reduced by shifting more dust particles to the internally mixed modes. This is consistent with the slight (non-significant) increase in immersion freezing occurring near the surface (Fig. 11d).

Compared to dust, BC initiates freezing only in very few cloud droplets (Fig. 11e). Furthermore, its influence is mainly restricted to high altitudes where temperatures are sufficiently low to initiate freezing. However, BC particles from ships are emitted near the surface. Although BC immersion freezing is somewhat enhanced near the surface (Fig. 11f), absolute changes are smaller than the decreases in contact freezing of dust. These findings lead to the conclusions that i) BC immersion freezing is largely not affected because of the low altitude of ship emissions, ii) even if it were, it would hardly matter because dust is by far the dominant INP, and iii) SO_2 emissions from ships lead to a slight shift from contact to immersion freezing near the surface, thus leading to a non-significant decrease in cloud ice at low altitudes.

3.2.3 Aerosol radiative forcings

The higher aerosol burdens due to ship emissions lead to significantly enhanced AOTs. Changes are on the same order of magnitude as the changes caused by additional sea salt and DMS emissions from 2004 to 2050. In contrast to the sea salt and DMS induced changes, which hardly affect aerosol absorption, ship emissions increase the aerosol absorption optical thickness pronouncedly. This is not surprising since OC and predominantely BC are important absorbers of sunlight.

In late summer, the SW component clearly dominates changes in the net aerosol radiative forcing. Under clear-sky conditions, the ship emissions induce a pronounced cooling (Fig. 12b). This cooling reverses to a non-significant warming under all-sky conditions (Fig. 12d). Again, this shows that the scattering of aerosol particles becomes less important when the scattering of clouds is considered as well.

In early autumn, changes in the SW component still dominate the aerosol radiative forcing in the region of shipping activity under clear-sky conditions. However, increases in the LW effect can locally be as important (e.g. northwards of 80° N). Under all-sky conditions, the SW aerosol radiative forcing does not change significantly, whereas the LW aerosol radiative forcing shows small but significant increases over a large part of the Arctic. However, like in late summer, changes in the net aerosol radiative forcing are not significant except for averaged values north of 75° N (see Table 3).

In early autumn, the BC deposition on snow leads to a small but significant warming over part of the Arctic Ocean (at most $0.01 - 0.05\,\mathrm{W\,m^{-2}}$; see Fig. 13d). Although these changes are pronounced in relative terms, they are more than one order of magnitude lower in absolute terms compared to the cooling by clouds, which is discussed in the next section: averaged

Atmos. Chem. Phys. Discuss., https://doi.org/10.5194/acp-2017-1007
Manuscript under review for journal Atmos. Chem. Phys.
Discussion started: 9 November 2017

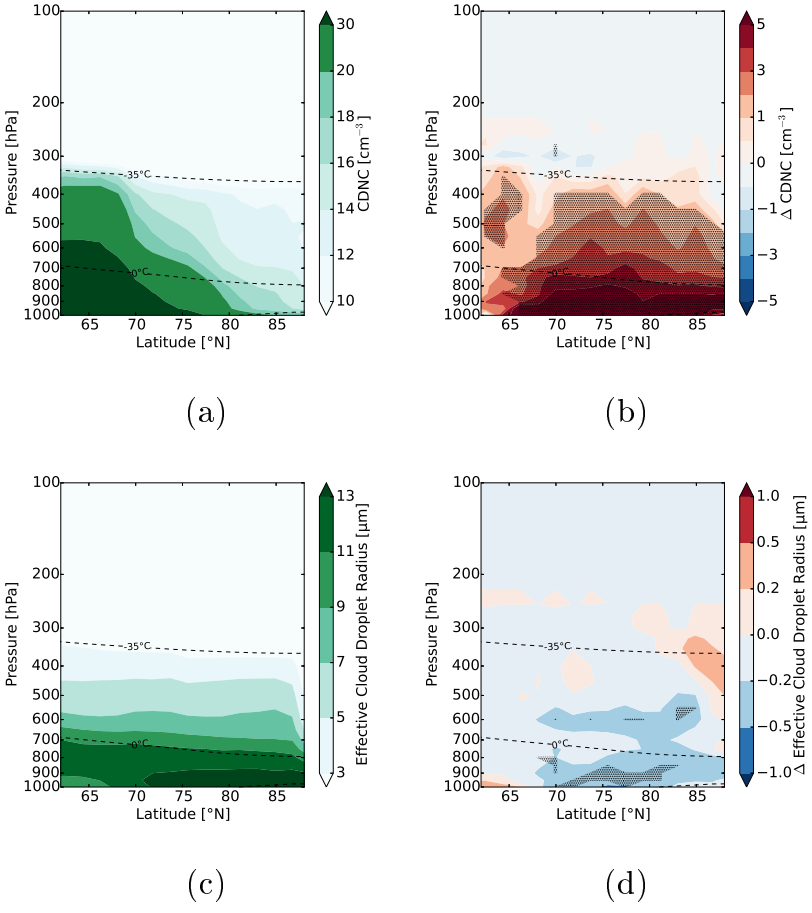

Figure 10. CDNC and effective cloud droplet radius in late summer (Jul/Aug): (a)/(c) show the absolute values for 2050 (reference), (b)/(d) the difference between a simulation with enhanced ship emissions and the reference simulation (difference between **arctic_2050_shipping** and **arctic_2050**). Stippled areas are significant at the 95% confidence level. The dashed lines show the 0°C- and the -35°C-isotherms.

between 60° and 90° N, deposited BC causes a warming of $0.018\,\mathrm{W\,m^{-2}}$ in late summer, while the SW CRE induces a cooling of $0.99\,\mathrm{W\,m^{-2}}$ (Table 2).

Atmos. Chem. Phys. Discuss., https://doi.org/10.5194/acp-2017-1007
Manuscript under review for journal Atmos. Chem. Phys.
Discussion started: 9 November 2017

3.2.4 Cloud radiative effects

In late summer, aerosol particles from ships lead to more but smaller cloud droplets, which reflect more solar radiation. Thus, we see an enhanced cooling effect of clouds in most areas where the CDNC burden increases (Fig. 13b, d), i.e. the SW CRE becomes more negative ($\approx 2-20\,\mathrm{W\,m^{-2}}$). Changes in the LW CRE are smaller in terms of absolute amount and not as consistently spatially correlated with ship emissions. However, changes are not significant, neither in the SW nor in the LW. We additionally analysed the different contributions to the CREs from cloud cover, cloud top altitude, and cloud thickness (see Fig. 14; the residual in (g) and (h) shows what can be attributed to neither cloud cover, nor cloud top altitude, nor cloud thickness). While the CRE caused by changes in cloud cover and cloud top altitude is not significant (Fig. 14a-d), the increase in cloud optical thickness leads to significant decreases and increases in the SW and LW CRE, respectively (Fig. 14e, f). Averaged between 75° and $90^\circ\,\mathrm{N}$, the increased optical thickness changes the SW CRE by $-2.89\,\mathrm{W\,m^{-2}}$ and LW CRE by $0.27\,\mathrm{W\,m^{-2}}$ in late summer. When we partition the contributions from low and free-tropospheric clouds (defined as clouds with a cloud top altitude below/above the altitude of $680\,\mathrm{hPa}$), we find that significant changes induced by cloud optical thickness only occur in low clouds. This is not surprising considering that the ship emissions occur near the surface. The increases in low cloud optical thickness change the SW and LW CRE by $-2.10\,\mathrm{W\,m^{-2}}$ and $0.08\,\mathrm{W\,m^{-2}}$, respectively.

To summarise, ship emissions lead to a significant but weak warming in early autumn caused by absorption of deposited BC on snow. In contrast, the direct impact of aerosol particles on the net radiation is not significant. The changes in CREs are also not significant but indicate that aerosol particles seem to enhance the cooling effect of clouds in late summer. This is confirmed when we partition the CREs from different components: we find no significant radiative changes induced by changing cloud top altitude or cloud cover, but the cloud optical thickness increases and leads to a significant net cooling. Due to the large variability in clouds (e.g. cloud cover), we do not find a significant signal when looking at all effects together. Since the cooling induced by aerosol-cloud interactions exceeds the warming of deposited BC by at least one order of magnitude, ship emissions can be expected to overall induce a local cooling.

Atmos. Chem. Phys. Discuss., https://doi.org/10.5194/acp-2017-1007
Manuscript under review for journal Atmos. Chem. Phys.
Discussion started: 9 November 2017

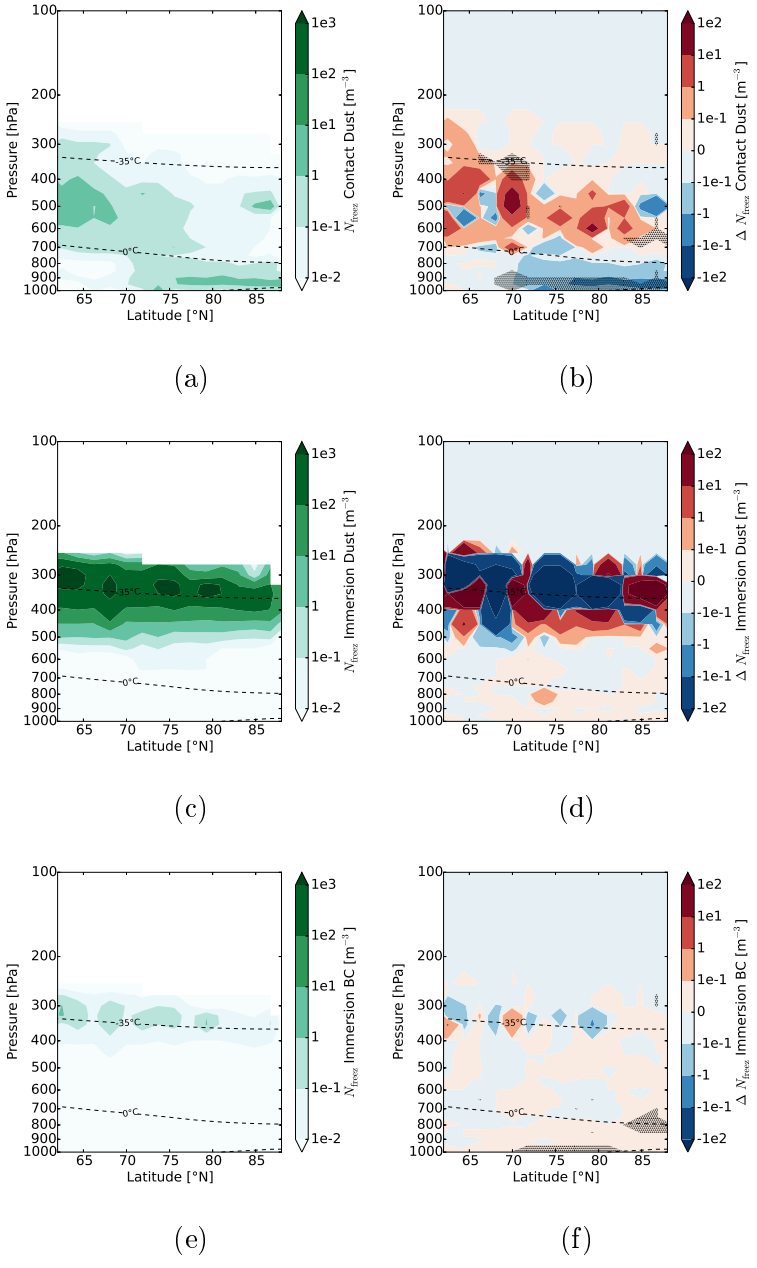

Figure 11. Number of cloud droplets frozen heterogeneously (N_{freez}) in 2050: (a)/(b) contact freezing by dust, (c)/(d) immersion freezing by dust, (e)/(f) immersion freezing by black carbon in late summer (Jul/Aug). On the left side, absolute values for 2050 (reference) are shown. On the right side, the difference between a simulation with enhanced ship emissions and the reference simulation is displayed (difference between **arctic_2050_shipping** and **arctic_2050**). Note that the colorbar is logarithmic. Stippled areas are significant at the 95% confidence level. The dashed lines show the 0°C- and the -35°C-isotherms. Note that the shown isotherms are a zonal and temporal average, hence ice in mixed-phase clouds can exist at altitudes below the 0°C-isotherm and above the -35°C-isotherm.

Atmos. Chem. Phys. Discuss., https://doi.org/10.5194/acp-2017-1007
Manuscript under review for journal Atmos. Chem. Phys.
Discussion started: 9 November 2017

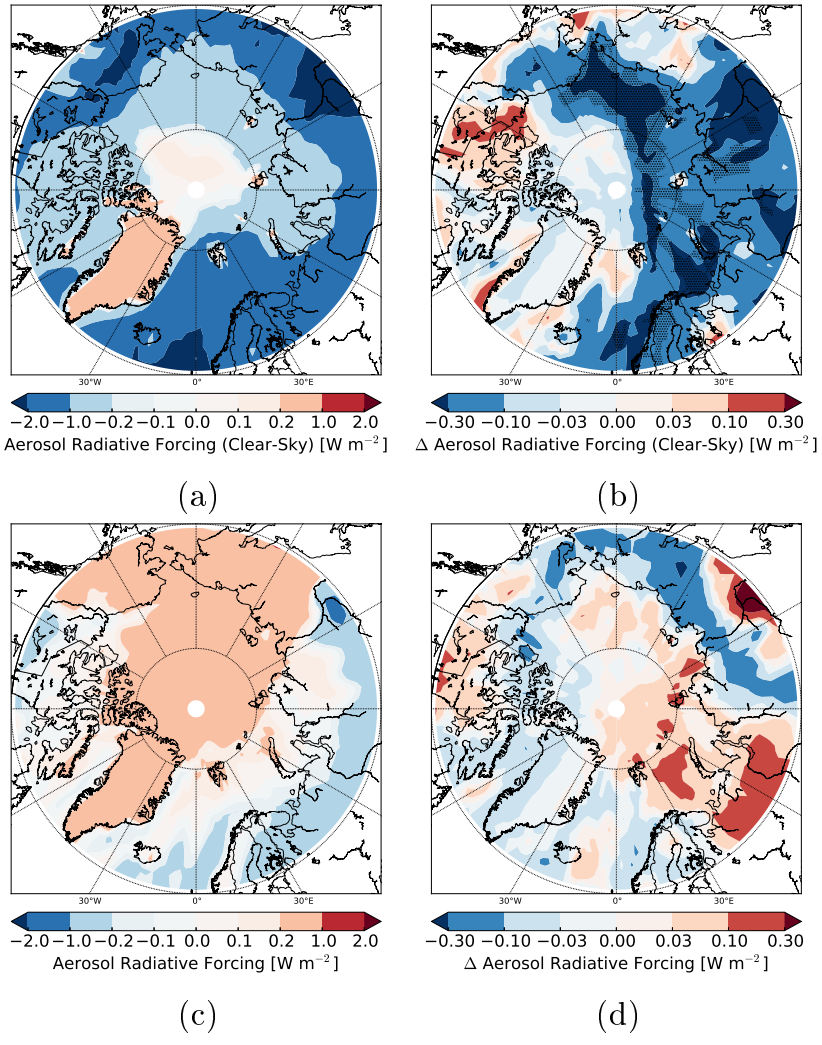

Figure 12. Aerosol radiative forcing in late summer (Jul/Aug) 2050: (a)/(b) under clear-sky and (c)/(d) under all-sky conditions. On the left side, absolute values for 2050 (reference) are shown. On the right side, the difference between a simulation with enhanced ship emissions and the reference simulation is displayed (difference between **arctic_2050_shipping** and **arctic_2050**). Stippled areas are significant at the 95% confidence level.

Atmos. Chem. Phys. Discuss., https://doi.org/10.5194/acp-2017-1007
Manuscript under review for journal Atmos. Chem. Phys.
Discussion started: 9 November 2017

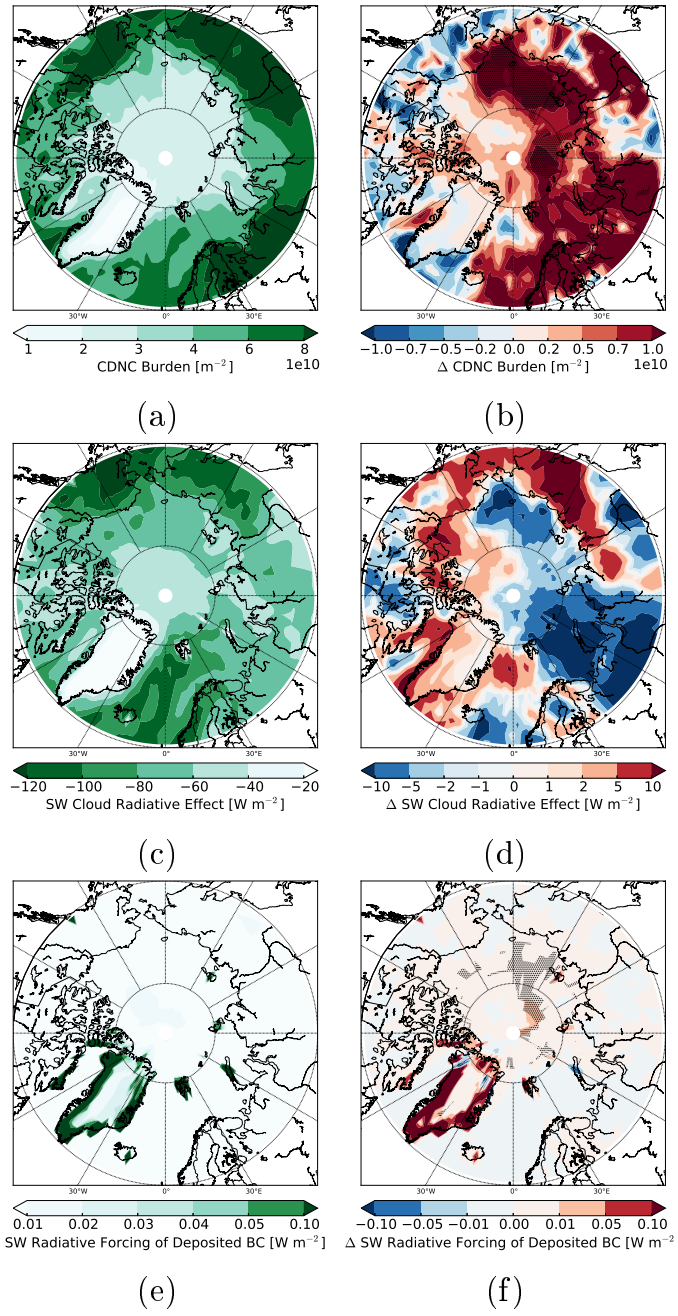

Figure 13. The impact of additional ship emissions in the Arctic on: (b) CDNC burden, (d) SW CRE, and (f) radiative effect of BC deposition on snow. In (a), (c), and (e), the reference without additional ship emissions is shown (**arctic_2050**). Stippled areas are significant at the 95% confidence level. (a) to (d) are shown for late summer (Jul/Aug), (e) and (f) for early autumn (Sep/Oct; seasons where pronounced changes occur).

Atmos. Chem. Phys. Discuss., https://doi.org/10.5194/acp-2017-1007
Manuscript under review for journal Atmos. Chem. Phys.
Discussion started: 9 November 2017

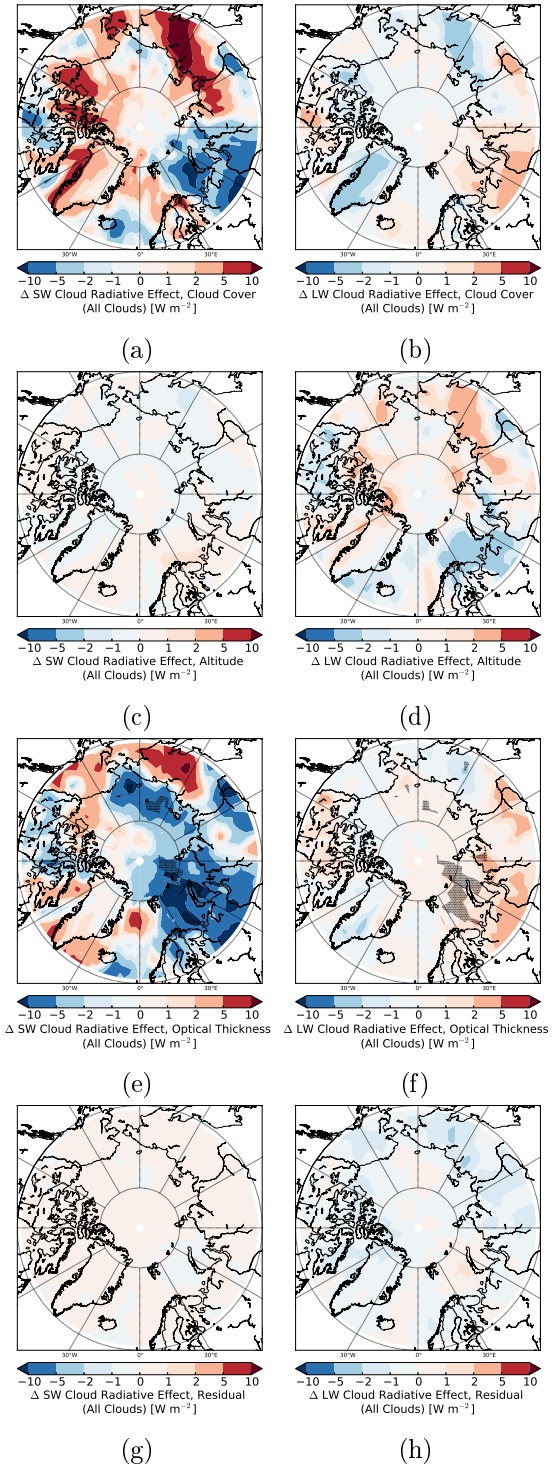

Figure 14. Different contributions to the SW (left) and LW (right) CREs in late summer (Jul/Aug): contribution from changes in (a)/(b) cloud cover, (c)/(d) cloud top altitude, and (e)/(f) cloud optical thickness. In (g)/(h), the residual is shown, which cannot be attributed to one of the three mentioned contributions (would ideally be zero). Stippled areas are significant at the 95% confidence level.

Atmos. Chem. Phys. Discuss., https://doi.org/10.5194/acp-2017-1007
Manuscript under review for journal Atmos. Chem. Phys.
Discussion started: 9 November 2017

4 Summary and conclusions

The main goal of this work was to analyse aerosol-cloud, aerosol-radiation, and cloud-radiation interactions in a warming Arctic when sea ice extent diminishes in late summer and early autumn. Simulations with ECHAM6-HAM2 were conducted for the years 2004 and 2050. We also estimated the impact of enhanced future Arctic shipping activity on climate.

Our results suggest that the future decrease in summer Arctic SIC will significantly increase aerosol burdens in the Arctic due to enhanced emissions of sea salt as well as DMS. The increase in CCN will lead to enhanced CDNCs. Furthermore, not only the number concentration but also the size of cloud droplets will generally increase because of higher specific humidities leading to thicker clouds. In late summer, the net CRE at the TOA will become more negative mainly because of the decrease in surface albedo associated with melting of sea ice. Also the aerosol radiative forcing will decrease as a consequence of sea ice melting and enhanced aerosol optical thickness in late summer and early autumn. The decrease in both net CRE and aerosol radiative forcing (negative temperature feedbacks) might delay Arctic warming to some extent.

Arctic ship emissions related to transport and oil/gas extraction have a negligible impact on clouds and radiation. Only when we increase the ship emissions of Peters et al. (2011) by a factor of ten is the signal-to-noise ratio sufficiently large to detect ship-induced changes. In this case, the AOT significantly increases on the same order of magnitude as natural AOT changes from 2004 to 2050. The net aerosol radiative forcing shows only minor changes in the presence of clouds, though. An increase in BC deposition on snow leads to local warming in early autumn. Meanwhile, a Twomey effect induces a cooling in late summer. Although this Twomey effect is statistically only significant for radiative effects associated with changes in cloud optical thickness, the magnitude of changes in radiation are considerably larger than those induced by the deposition of BC on snow, implying that ship emissions might overall induce a cooling.

Compared to other changes (such as the decrease in surface albedo or the increase in natural aerosol emissions), ship emissions seem to have a small effect on climate considering that we scaled the emissions up by one order of magnitude. Such high Arctic ship emissions are more likely to occur in years later than 2050 when large population and economic demand could lead to further increases in transit and petroleum-related shipping. However, even though this study suggests that Arctic ship emissions might have a negligible or slightly beneficial impact on climate, they will also increase air pollution and might disturb local flora and fauna. More studies are required to confirm or object the results found in this work as well as to explore further ship-related environmental impacts.

5 Code availability

The code is available upon request.

6 Data availability

The data is available upon request.

Atmos. Chem. Phys. Discuss., https://doi.org/10.5194/acp-2017-1007
Manuscript under review for journal Atmos. Chem. Phys.
Discussion started: 9 November 2017

Atmospheric Chemistry and Physics Discussions

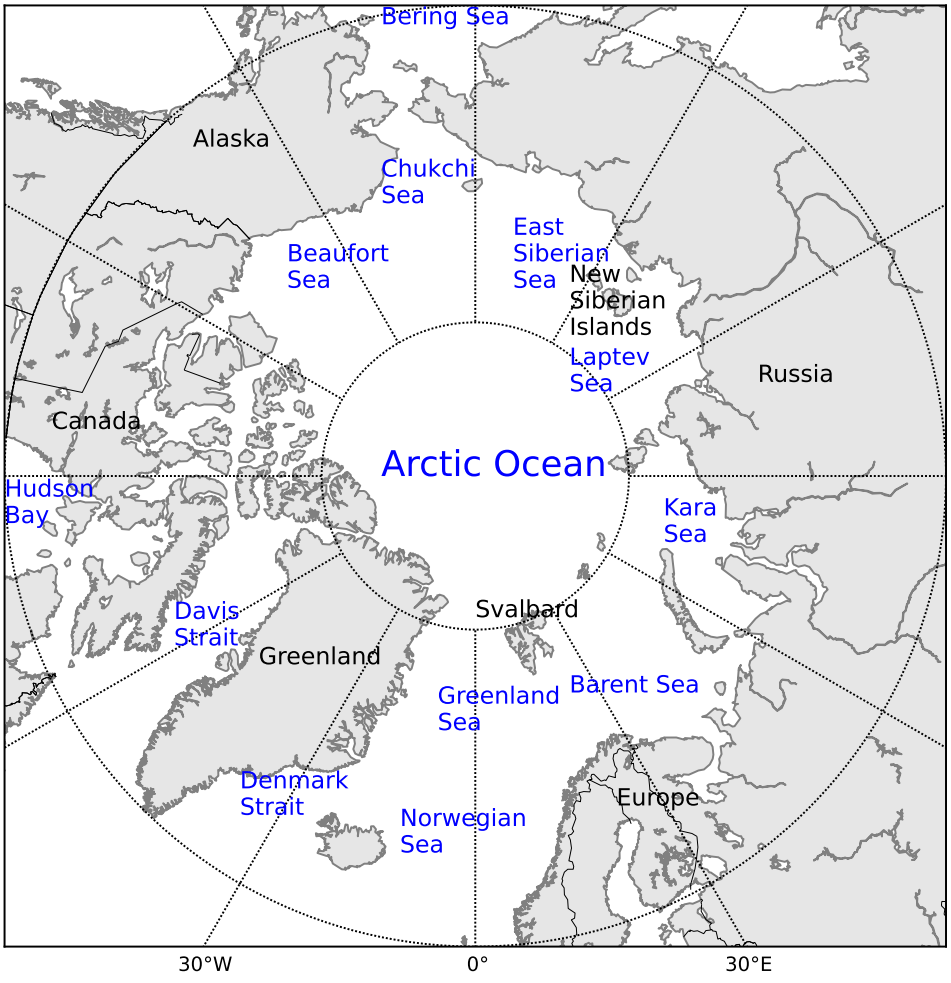

Figure A1. The Arctic Ocean and regional seas are labelled in blue, land masses in black.

Appendix A: Map of Arctic Seas

As a help for readers not familiar with the Arctic Ocean, Fig. A1 shows its most important regional seas. Furthermore, some land masses are labelled for better orientation.

Atmos. Chem. Phys. Discuss., https://doi.org/10.5194/acp-2017-1007
Manuscript under review for journal Atmos. Chem. Phys.
Discussion started: 9 November 2017

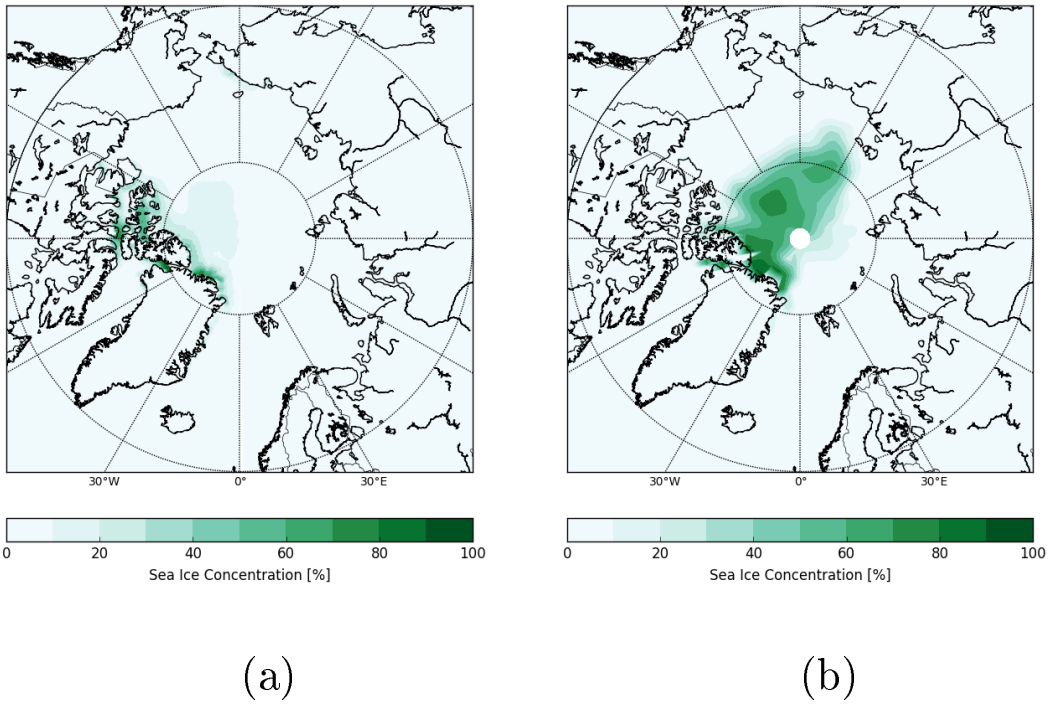

Figure A2. SIC in 2050 for (a) NCAR-CCSM3 in September (average over 5 ensemble members) and (b) MPI-ESM in October (the ensemble member used in this study).

Appendix B: Comparison of sea ice between MPI-ESM and NCAR-CCSM3

Here we compare the sea ice used as input for the study of Peters et al. (2011) with our prescribed sea ice from MPI-ESM. With that we want to ensure that the ship emissions – which explicitly depend on the sea ice thickness and concentration – are compatible with the sea ice used in our study. Peters et al. (2011) used a 5-year running average of the NCAR-CCSM3 model to calculate future sea ice conditions (scenario A2). Instead of averaging over years, we calculated the mean over the 5 ensemble members of NCAR-CCSM3 from CMIP3 for our comparison, which should give similar results. For their calculations, Peters et al. (2011) chose the months March, June, September, and December to represent each season. In our model, we prescribe the sea ice monthly because this is more realistic. Therefore, we will compare the sea ice in July from MPI-ESM with the sea ice in June from NCAR-CCSM3 and the sea ice from August to October from MPI-ESM with the sea ice in September from NCAR-CCSM3. For this comparison, we will focus on the regions where most Arctic ship emissions are projected.

The sea ice thickness is generally thinner in MPI-ESM than in NCAR-CCSM3. The opposite is the case for the sea ice extent, which is larger in MPI-ESM than in NCAR-CCSM3. In August and October, the SIC in MPI-ESM is higher than the NCAR-CCSM3 September value (used by Peters et al. (2011) for August, September, and October). At the locations of the ship

Atmos. Chem. Phys. Discuss., https://doi.org/10.5194/acp-2017-1007
Manuscript under review for journal Atmos. Chem. Phys.
Discussion started: 9 November 2017

tracks, differences are most pronounced north of the New Siberian Islands, where the SIC reaches up to 60-70% in MPI-ESM, whereas basically no sea ice is left in NCAR-CCSM3 (see Fig. A2). However, with an extended use of ice breakers, ships can pass despite the higher SIC. Furthermore, the area where this larger SIC for MPI-ESM occurs is rather small, as the SIC in MPI-ESM rapidly decreases towards the New Siberian Islands and the Russian coast. By slightly changing the shipping routes, most of the additional expenses linked to SIC (i.e. to ice breakers, which are included in the cost-benefit analysis of Peters et al., 2011) would be saved. We therefore expect that costs associated with breaking and/or bypassing sea ice are small and should not considerably change the ship emissions derived by Peters et al. (2011).

Appendix C: Significance test for cloud feedback

The cloud feedback is calculated using radiative kernels. These kernels are calculated as *differences* of two simulations, here represented by the vectors $\boldsymbol{a} = \begin{pmatrix} a_1 \\ a_2 \\ a_3 \\ \dots \\ a_n \end{pmatrix}$ and $\boldsymbol{b} = \begin{pmatrix} b_1 \\ b_2 \\ b_3 \\ \dots \\ b_n \end{pmatrix}$, where n is the number of samples. In our case, we could not simply use a one sample t-test upon the differences $\boldsymbol{a} - \boldsymbol{b}$ because the differences are calculated from 10 *independent* samples (i.e. years) with different standard deviations for the different simulations. Instead, we reconstructed from the following differences the standard deviation of $\boldsymbol{a}$, the standard deviation of $\boldsymbol{b}$, and the difference between the means of $\boldsymbol{b}$ and $\boldsymbol{a}$:

- For standard deviation of $\boldsymbol{a}$: calculate standard devation of $\begin{pmatrix} b_1 - a_1 \\ b_1 - a_2 \\ \dots \\ b_1 - a_n \end{pmatrix}$.
- For standard deviation of $\boldsymbol{b}$: calculate standard devation of $\begin{pmatrix} a_1 - b_1 \\ a_1 - b_2 \\ \dots \\ a_1 - b_n \end{pmatrix}$.
- For difference between the means of $\boldsymbol{b}$ and $\boldsymbol{a}$: $\frac{b_1+b_2+\dots+b_n}{n} - \frac{(a_1+a_2+\dots+a_n)}{n} = \frac{b_1-a_1+b_2-a_2+\dots+b_n-a_n}{n}$, i.e. we calculated the kernels between b_1 and a_1, ..., b_n and a_n and calculated the average of these differences.

With this information, we could calculate the p-values using the Welch's test for each gridpoint and control the FDR as described in Sect. 2.5.

Competing interests. The authors confirm that they have no conflict of interest.

Acknowledgements. The research leading to these results has received funding from the European Union's Seventh Framework Programme (FP7/2007-2013) project BACCHUS under grant agreement no. 603445. This work was also supported by a grant from the Swiss National Supercomputing Centre (CSCS) under project ID s652. We are very grateful to Stig B. Dalsøren and Glenn P. Peters, who kindly gave access to their ship emission inventories. Furthermore, we thank Sylvaine Ferrachat, who set up the simulations for the (unpublished) precursor study of this paper. We acknowledge the international modeling groups for providing their data for analysis, and the Program for Climate Model Diagnosis and Intercomparison (PCMDI) for collecting and archiving the model data. In this context, we also thank Jan Sedlacek for his effort to process the CMIP5 data set. The ECHAM-HAMMOZ model is developed by a consortium composed of ETH Zürich, Max Planck Institut für Meteorologie, Forschungszentrum Jülich, University of Oxford, the Finnish Meteorological Institute, and the Leibniz Institute for Tropospheric Research, and managed by the Center for Climate Systems Modeling (C2SM) at ETH Zürich. Concerning the model development, special thanks go to the "Fire in the Earth System" Group of Silvia Kloster (part of the Emmy Noether Junior Research Group; MPI) for implementing the BC deposition over land in ECHAM. We are also grateful to Ina Tegen and Stefan Barthel, who implemented the used sea salt parameterisation into ECHAM-HAM.

References

Abdul-Razzak, H. and Ghan, S. J.: A parameterization of aerosol activation: 2. Multiple aerosol types, J. Geophys. Res.-Atmos., 105, 6837–6844, doi:10.1029/1999JD901161, 2000.

Abe, M., Nozawa, T., Ogura, T., and Takata, K.: Effect of retreating sea ice on Arctic cloud cover in simulated recent global warming, Atmos. Chem. Phys., 16, 14 343–14 356, doi:10.5194/acp-16-14343-2016, 2016.

Albrecht, B.: Aerosols, Cloud Microphysics, and Fractional Cloudiness, Science, 245, 1227–1230, doi:10.1126/science.245.4923.1227, 1989.

Alterskjær, K., Kristjánsson, J. E., and Hoose, C.: Do anthropogenic aerosols enhance or suppress the surface cloud forcing in the Arctic?, J. Geophys. Res., 115, doi:10.1029/2010jd014015, 2010.

Becagli, S., Lazzara, L., Marchese, C., Dayan, U., Ascanius, S., Cacciani, M., Caiazzo, L., Biagio, C. D., Iorio, T. D., di Sarra, A., Eriksen, P., Fani, F., Giardi, F., Meloni, D., Muscari, G., Pace, G., Severi, M., Traversi, R., and Udisti, R.: Relationships linking primary production, sea ice melting, and biogenic aerosol in the Arctic, Atmos. Environ., 136, 1 – 15, doi:10.1016/j.atmosenv.2016.04.002, 2016.

Bigg, E. K. and Leck, C.: Cloud-active particles over the central Arctic Ocean, J. Geophys. Res.-Atmos., 106, 32 155–32 166, doi:10.1029/1999JD901152, 2001.

Boucher, O., Randall, D., Artaxo, P., Bretherton, C., Feingold, G., Forster, P., Kerminen, V.-M., Kondo, Y., Liao, H., Lohmann, U., Rasch, P., Satheesh, S., Sherwood, S., Stevens, B., and Zhang, X.: Clouds and Aerosols. In: Climate Change 2013: The Physical Science Basis. Contribution of Working Group I to the Fifth Assessment Report of the Intergovernmental Panel on Climate Change [Stocker, T.F., D. Qin, G.-K. Plattner, M. Tignor, S.K. Allen, J. Boschung, A. Nauels, Y. Xia, V. Bex and P.M. Midgley (eds.)]., Cambridge University Press, Cambridge, United Kingdom and New York, NY, USA., 2013.

Browse, J., Carslaw, K. S., Mann, G. W., Birch, C. E., Arnold, S. R., and Leck, C.: The complex response of Arctic aerosol to sea-ice retreat, Atmos. Chem. Phys., 14, 7543–7557, doi:10.5194/acp-14-7543-2014, 2014.

Chen, Y., Aires, F., Francis, J. A., and Miller, J. R.: Observed Relationships between Arctic Longwave Cloud Forcing and Cloud Parameters Using a Neural Network, J. Climate, 19, 4087–4104, doi:10.1175/JCLI3839.1, 2006.

Cheng, T., Peng, Y., Feichter, J., and Tegen, I.: An improvement on the dust emission scheme in the global aerosol-climate model ECHAM5-HAM, Atmos. Chem. Phys., 8, 1105–1117, doi:10.5194/acp-8-1105-2008, 2008.

Christensen, M. W., Suzuki, K., Zambri, B., and Stephens, G. L.: Ship track observations of a reduced shortwave aerosol indirect effect in mixed-phase clouds, Geophy. Res. Lett., 41, 6970–6977, doi:10.1002/2014GL061320, 2014.

Collins, M., Knutti, R., Arblaster, J., Dufresne, J.-L., Fichefet, T., Friedlingstein, P., Gao, X., Gutowski, W., Johns, T., Krinner, G., Shongwe, M., Tebaldi, C., Weaver, A., and Wehner, M.: Long-term Climate Change: Projections, Commitments and Irreversibility. In: Climate Change 2013: The Physical Science Basis. Contribution of Working Group I to the Fifth Assessment Report of the Intergovernmental Panel on Climate Change [Stocker, T.F., D. Qin, G.-K. Plattner, M. Tignor, S.K. Allen, J. Boschung, A. Nauels, Y. Xia, V. Bex and P.M. Midgley (eds.)]., Cambridge University Press, Cambridge, United Kingdom and New York, NY, USA., 2013.

Corbett, J. J., Lack, D. A., Winebrake, J. J., Harder, S., Silberman, J. A., and Gold, M.: Arctic shipping emissions inventories and future scenarios, Atmos. Chem. Phys., 10, 9689–9704, doi:10.5194/acp-10-9689-2010, 2010.

Croft, B., Lohmann, U., Martin, R. V., Stier, P., Wurzler, S., Feichter, J., Hoose, C., Heikkilä, U., van Donkelaar, A., and Ferrachat, S.: Influences of in-cloud aerosol scavenging parameterizations on aerosol concentrations and wet deposition in ECHAM5-HAM, Atmos. Chem. Phys., 10, 1511–1543, doi:10.5194/acp-10-1511-2010, 2010.

Dalsøren, S. B., Eide, M. S., Endresen, Ø., Mjelde, A., Gravir, G., and Isaksen, I. S. A.: Update on emissions and environmental impacts from the international fleet of ships: the contribution from major ship types and ports, Atmos. Chem. Phys., 9, 2171–2194, doi:10.5194/acp-9-2171-2009, 2009.

Dentener, F., Kinne, S., Bond, T., Boucher, O., Cofala, J., Generoso, S., Ginoux, P., Gong, S., Hoelzemann, J. J., Ito, A., Marelli, L., Penner, J. E., Putaud, J.-P., Textor, C., Schulz, M., van der Werf, G. R., and Wilson, J.: Emissions of primary aerosol and precursor gases in the years 2000 and 1750 prescribed data-sets for AeroCom, Atmos. Chem. Phys., 6, 4321–4344, doi:10.5194/acp-6-4321-2006, 2006.

Deshpande, C. and Kambra, A.: Physical properties of the arctic summer aerosol particles in relation to sources at Ny-Alesund, Svalbard, J. Earth Syst. Sci., 123, 201–212, doi:10.1007/s12040-013-0373-0, 2014.

Eckhardt, S., Hermansen, O., Grythe, H., Fiebig, M., Stebel, K., Cassiani, M., Baecklund, A., and Stohl, A.: The influence of cruise ship emissions on air pollution in Svalbard a harbinger of a more polluted Arctic?, Atmos. Chem. Phys., 13, 8401–8409, doi:10.5194/acp-13-8401-2013, 2013.

Flanner, M.: Arctic climate sensitivity to local black carbon, J. Geophys. Res., 118, 1840–1851, doi:10.1002/jgrd.50176, 2013.

Flanner, M. G., Zender, C. S., Randerson, J. T., and Rasch, P. J.: Present-day climate forcing and response from black carbon in snow, J. Geophys. Res.-Atmos., 112, doi:10.1029/2006JD008003, d11202, 2007.

Garrett, T. J. and Zhao, C.: Increased Arctic cloud longwave emissivity associated with pollution from mid-latitudes, Nature, 440, 787–789, doi:10.1038/nature04636, 2006.

Gong, S. L.: A parameterization of sea-salt aerosol source function for sub- and super-micron particles, Global Biogeochem. Cy., 17, doi:10.1029/2003GB002079, 1097, 2003.

Hoose, C., Lohmann, U., Erdin, R., and Tegen, I.: The global influence of dust mineralogical composition on heterogeneous ice nucleation in mixed-phase clouds, Environ. Res. Lett., 3, 025 003, doi:10.1088/1748-9326/3/2/025003, 2008.

Intrieri, J. M., Fairall, C., Shupe, M., Persson, P., E.L., A., Guest, P., and Moritz, R.: An annual cycle of Arctic surface cloud forcing at SHEBA, J. Geophys. Res., 107, doi:10.1029/2000jc000439, 2002.

Jackson, R. C., McFarquhar, G. M., Korolev, A. V., Earle, M. E., Liu, P. S. K., Lawson, R. P., Brooks, S., Wolde, M., Laskin, A., and Freer, M.: The dependence of ice microphysics on aerosol concentration in arctic mixed-phase stratus clouds during ISDAC and M-PACE, J. Geophys. Res., 117, doi:10.1029/2012jd017668, 2012.

Kanji, Z. A., Ladino, L. A., Wex, H., Boose, Y., Burkert-Kohn, M., Cziczo, D. J., and Krämer, M.: Overview of Ice Nucleating Particles, Meteor. Mon., 58, 1.1–1.33, doi:10.1175/AMSMONOGRAPHS-D-16-0006.1, 2017.

Kettle, A. and Andreae, M.: Flux of dimethylsulfide from the oceans: A comparison of updated data sets and flux models, J. Geophys. Res., 105, 26 793–26 808, doi:10.1029/2000JD900252, 2000.

Kloster, S., Six, K. D., Feichter, J., Maier-Reimer, E., Roeckner, E., Wetzel, P., Stier, P., and Esch, M.: Response of dimethylsulfide (DMS) in the ocean and atmosphere to global warming, J. Geophys. Res.-Biogeo., 112, doi:10.1029/2006JG000224, g03005, 2007.

Lamarque, J.-F., Bond, T. C., Eyring, V., Granier, C., Heil, A., Klimont, Z., Lee, D., Liousse, C., Mieville, A., Owen, B., Schultz, M. G., Shindell, D., Smith, S. J., Stehfest, E., Van Aardenne, J., Cooper, O. R., Kainuma, M., Mahowald, N., McConnell, J. R., Naik, V., Riahi, K., and van Vuuren, D. P.: Historical (1850–2000) gridded anthropogenic and biomass burning emissions of reactive gases and aerosols: methodology and application, Atmos. Chem. Phys., 10, 7017–7039, doi:10.5194/acp-10-7017-2010, 2010.

Lance, S., Shupe, M. D., Feingold, G., Brock, C. A., Cozic, J., Holloway, J. S., Moore, R. H., Nenes, A., Schwarz, J. P., Spackman, J. R., and et al.: Cloud condensation nuclei as a modulator of ice processes in Arctic mixed-phase clouds, Atmos. Chem. Phys., 11, 8003–8015, doi:10.5194/acp-11-8003-2011, 2011.

Laszlo, I. and Pinker, R.: Shortwave Cloud-Radiative Forcing at the Top of the Atmosphere, at the Surface and of the Atmospheric Column As Determined From ISCCP C1 Data, J. Geophys. Res., 98, 2703–2713, 1993.

Leaitch, W. R., Korolev, A., Aliabadi, A. A., Burkart, J., Willis, M. D., Abbatt, J. P. D., Bozem, H., Hoor, P., Köllner, F., Schneider, J., Herber, A., Konrad, C., and Brauner, R.: Effects of 20–100 nm particles on liquid clouds in the clean summertime Arctic, Atmos. Chem. Phys., 16, 11 107–11 124, doi:10.5194/acp-16-11107-2016, 2016.

Liou, K.: An Introduction to Atmospheric Radiation, International Geophysics, 84, 1–583, 2002.

Liu, Y., Key, J. R., Liu, Z., Wang, X., and Vavrus, S. J.: A cloudier Arctic expected with diminishing sea ice, Geophy. Res. Lett., 39, doi:10.1029/2012GL051251, l05705, 2012.

Lohmann, U.: A glaciation indirect aerosol effect caused by soot aerosols, Geophy. Res. Lett., 29, 11–1–11–4, doi:10.1029/2001GL014357, 2002.

Lohmann, U. and Feichter, J.: Global indirect aerosol effects: a review, Atmos. Chem. Phys., 5, 715–737, doi:10.5194/acp-5-715-2005, 2005.

Lohmann, U., Spichtinger, P., Jess, S., Peter, T., and Smit, H.: Cirrus cloud formation and ice supersaturated regions in a global climate model, Environmental Research Letters, 3, 045 022, doi:10.1088/1748-9326/3/4/045022, 2008.

Long, M. S., Keene, W. C., Kieber, D. J., Erickson, D. J., and Maring, H.: A sea-state based source function for size- and composition-resolved marine aerosol production, Atmos. Chem. Phys., 11, 1203–1216, doi:10.5194/acp-11-1203-2011, 2011.

Mauritsen, T., Sedlar, J., Tjernström, M., Leck, C., Martin, M., Shupe, M., Sjogren, S., Sierau, B., Persson, P. O. G., Brooks, I. M., and et al.: An Arctic CCN-limited cloud-aerosol regime, Atmos. Chem. Phys., 11, 165–173, doi:10.5194/acp-11-165-2011, 2011.

McFarquhar, G. M., Ghan, S., Verlinde, J., Korolev, A., Strapp, J. W., Schmid, B., Tomlinson, J. M., Wolde, M., Brooks, S. D., Cziczo, D., and et al.: Indirect and Semi-direct Aerosol Campaign, Bull. Amer. Meteor. Soc., 92, 183–201, doi:10.1175/2010bams2935.1, 2011.

McKuin, B. and Campbell, J. E.: Emissions and climate forcing from global and Arctic fishing vessels, J. Geophys. Res.-Atmos., 121, 1844–1858, doi:10.1002/2015JD023747, 2015JD023747, 2016.

Monahan, E., Spiel, D., and Davidson, K.: A model of marine aerosol generation via whitecaps and wave disruption, in: Oceanic whitecaps and their role in air-sea exchange, vol. 2 of *Oceanographic Sciences Library*, D. Reidel Publishing Company, Norwell, Massachusetts, 1986.

Mårtensson, E. M., Nilsson, E. D., de Leeuw, G., Cohen, L. H., and Hansson, H.-C.: Laboratory simulations and parameterization of the primary marine aerosol production, J. Geophys. Res.-Atmos., 108, doi:10.1029/2002JD002263, 4297, 2003.

Nightingale, P., Malin, G., Law, C., Watson, A., Liss, P., Liddicoat, M., Boutin, J., and Upstill-Goddard, R.: In situ evaluation of air-sea gas exchange parameterizations using novel conservative and volatile tracers, Global Biogeochem. Cy., 14, 373–387, doi:10.1029/1999GB900091, 2000.

Palm, S. P., Strey, S. T., Spinhirne, J., and Markus, T.: Influence of Arctic sea ice extent on polar cloud fraction and vertical structure and implications for regional climate, J. Geophys. Res., 115, doi:10.1029/2010jd013900, 2010.

Paxian, A., Eyring, V., Beer, W., Sausen, R., and Wright, C.: Present-Day and Future Global Bottom-Up Ship Emission Inventories Including Polar Routes, Environ. Sci. Technol., 44, 1333–1339, doi:10.1021/es9022859, 2010.

Peters, G. P., Nilssen, T. B., Lindholt, L., Eide, M. S., Glomsrød, S., Eide, L. I., and Fuglestvedt, J. S.: Future emissions from shipping and petroleum activities in the Arctic, Atmos. Chem. Phys., 11, 5305–5320, doi:10.5194/acp-11-5305-2011, 2011.

Peters, K., Quaas, J., Stier, P., and Graßl, H.: Processes limiting the emergence of detectable aerosol indirect effects on tropical warm clouds in global aerosol-climate model and satellite data, Tellus B, 66, 24 054, doi:10.3402/tellusb.v66.24054, 2014.

Pithan, F. and Mauritsen, T.: Arctic amplification dominated by temperature feedbacks in contemporary climate models, Nature Geosci., 7, 181–184, doi:10.1038/ngeo2071, 2014.

Sant, V., Posselt, R., and Lohmann, U.: Prognostic precipitation with three liquid water classes in the ECHAM5-HAM GCM, Atmos. Chem. Phys., 15, 8717–8738, doi:10.5194/acp-15-8717-2015, 2015.

Shupe, M. D. and Intrieri, J. M.: Cloud Radiative Forcing of the Arctic Surface: The Influence of Cloud Properties, Surface Albedo, and Solar Zenith Angle, J. Climate, 17, 616–628, doi:10.1175/1520-0442(2004)017<0616:CRFOTA>2.0.CO;2, 2003.

Slagstad, D., Wassmann, P. F. J., and Ellingsen, I.: Physical constrains and productivity in the future Arctic Ocean, Frontiers in Marine Science, 2, 85, doi:10.3389/fmars.2015.00085, 2015.

Sofiev, M., Soares, J., Prank, M., de Leeuw, G., and Kukkonen, J.: A regional-to-global model of emission and transport of sea salt particles in the atmosphere, J. Geophys. Res.-Atmos., 116, doi:10.1029/2010JD014713, d21302, 2011.

Stevens, B., Giorgetta, M., Esch, M., Mauritsen, T., Crueger, T., Rast, S., Salzmann, M., Schmidt, H., Bader, J., Block, K., Brokopf, R., Fast, I., Kinne, S., Kornblueh, L., Lohmann, U., Pincus, R., Reichler, T., and Roeckner, E.: Atmospheric component of the MPI-M Earth System Model: ECHAM6, J. Adv. Model. Earth Sy., 5, 146–172, doi:10.1002/jame.20015, 2013.

Stier, P., Feichter, J., Kinne, S., Kloster, S., Vignati, E., Wilson, J., Ganzeveld, L., Tegen, I., Werner, M., Balkanski, Y., and et al.: The aerosol-climate model ECHAM5-HAM, Atmos. Chem. Phys., 5, 1125–1156, doi:10.5194/acp-5-1125-2005, 2005.

Stier, P., Seinfeld, J. H., Kinne, S., and Boucher, O.: Aerosol absorption and radiative forcing, Atmos. Chem. Phys., 7, 5237–5261, doi:10.5194/acp-7-5237-2007, 2007.

Struthers, H., Ekman, A. M. L., Glantz, P., Iversen, T., Kirkevåg, A., Mårtensson, E. M., Seland, O., and Nilsson, E. D.: The effect of sea ice loss on sea salt aerosol concentrations and the radiative balance in the Arctic, Atmos. Chem. Phys., 11, 3459–3477, doi:10.5194/acp-11-3459-2011, 2011.

Taylor, K., Williamson, D., and Zwiers, F.: PCMDI Report No. 60. The sea surface temperature and sea-ice concentration boundary conditions for AMIP II simulations, Tech. rep., University of California, Lawrence Livermore National Laboratory, 2000.

Tegen, I., Harrison, S. P., Kohfeld, K., Prentice, I. C., Coe, M., and Heimann, M.: Impact of vegetation and preferential source areas on global dust aerosol: Results from a model study, J. Geophys. Res., 107, 4576, doi:10.1029/2001JD000963, 2002.

Twomey, S.: Pollution and planetary albedo, Atmos. Environ., 8, 1251–1256, doi:10.1016/0004-6981(74)90004-3, 1974.

Twomey, S.: The Influence of Pollution on the Shortwave Albedo of Clouds, American Meteorological Society, 34, 1149–1152, doi:10.1175/1520-0469(1977)034<1149:TIOPOT>2.0.CO;2, 1977.

Vali, G.: Nucleation terminology, J. Aerosol Sci., 16, 575 – 576, doi:10.1016/0021-8502(85)90009-6, 1985.

Vancoppenolle, M., Bopp, L., Madec, G., Dunne, J., Ilyina, T., Halloran, P. R., and Steiner, N.: Future Arctic Ocean primary productivity from CMIP5 simulations: Uncertain outcome, but consistent mechanisms, Global Biogeochem. Cy., 27, 605–619, doi:10.1002/gbc.20055, 2013.

Vaughan, D., Comiso, J., Allison, I., Carrasco, I., Kaser, G., Kwok, R., Mote, P., Murray, T., Paul, F., Ren, J., Rignot, E., Solomina, O., Steffen, K., and Zhang, T.: Observations: Cryosphere. In: Climate Change 2013: The Physical Science Basis. Contribution of Working Group I to the Fifth Assessment Report of the Intergovernmental Panel on Climate Change [Stocker, T.F., D. Qin, G.-K. Plattner, M. Tignor, S.K. Allen, J. Boschung, A. Nauels, Y. Xia, V. Bex and P.M. Midgley (eds.)]., Cambridge University Press, Cambridge, United Kingdom and New York, NY, USA., 2013.

Walsh, J. E. and Chapman, W. L.: Arctic Cloud-Radiation-Temperature Associations in Observational Data and Atmospheric Reanalyses, J. Climate, 11, 3030–3045, doi:10.1175/1520-0442(1998)011<3030:ACRTAI>2.0.CO;2, 1998.

Warren, S. G. and Wiscombe, W. J.: Dirty snow after nuclear war, Nature, 313, 467–470, doi:10.1038/313467a0, 1985.

Wild, M., Hakuba, M. Z., Folini, D., Schär, C., and Long, C.: New estimates of the Earth radiation budget under cloud-free conditions and cloud radiative effects, AIP Conference Proceedings, 1810, 090 012, doi:10.1063/1.4975552, 2017.

Wilks, D. S.: "The Stippling Shows Statistically Significant Grid Points": How Research Results are Routinely Overstated and Overinterpreted, and What to Do about It, B. Am. Meteorol. Soc., 97, 2263–2273, doi:10.1175/BAMS-D-15-00267.1, 2016.

Yool, A., Popova, E. E., and Coward, A. C.: Future change in ocean productivity: Is the Arctic the new Atlantic?, J. Geophys. Res.-Oceans, 120, 7771–7790, doi:10.1002/2015JC011167, 2015.

Zelinka, M. D., Klein, S. A., and Hartmann, D. L.: Computing and Partitioning Cloud Feedbacks Using Cloud Property Histograms. Part I: Cloud Radiative Kernels, J. Climate, 25, 3715–3735, doi:10.1175/JCLI-D-11-00248.1, 2012.

Zelinka, M. D., Zhou, C., and Klein, S. A.: Insights from a refined decomposition of cloud feedbacks, Geophy. Res. Lett., 43, 9259–9269, doi:10.1002/2016GL069917, 2016GL069917, 2016.

Zhang, K., O'Donnell, D., Kazil, J., Stier, P., Kinne, S., Lohmann, U., Ferrachat, S., Croft, B., Quaas, J., Wan, H., and et al.: The global aerosol-climate model ECHAM-HAM, version 2: sensitivity to improvements in process representations, Atmos. Chem. Phys., 12, 8911–8949, doi:10.5194/acp-12-8911-2012, 2012.